UNCLASSIFIED

THIS PAGE IS UNCLASSIFIED

AD-453-253

MHD research, inc.

The attached paper will be delivered as a
20 minute presentation to the 5th Symposium on
"Engineering Aspects of Magnetohydrodynamics"
at Massachusetts Institute of Technology:
April 1 and 2, 1964

DDC

OCT 31 1967

GENERATION OF SHORT DURATION PULSES IN LINEAR MHD GENERATORS[*]

Malcolm S. Jones, Jr., Charles N. McKinnon and Vernon H. Blackman

MHD Research, Inc.

Newport Beach, California

1. Introduction

One of the most interesting aspects of MHD power conversion is the potential for obtaining high power densities in the energy conversion section. For example, in experiments with a small size, explosive driven MHD generator, reported in this paper, power densities as high as 2×10^{10} watts per cubic meter have been obtained. This potential offers many possibilities for an MHD generator, which would be relatively small in size - light in weight per unit output, as a source of pulsed electric power, or more descriptively, pulsed electric energy.

Preliminary results obtained with the explosive driven MHD generator were presented in Reference 1. The present paper gives additional data on these experiments and presents data from a series of experiments conducted in two different size channels under a variety of initial conditions. These results are compared with various theoretical models.

The peak power which has been generated by this technique is 23 MW (Reference 2). This output was evidenced as an output current of 30 kA into a 25.8 milliohm resistive load to produce a terminal voltage of 770 volts. The MHD channel used in these experiments was 1 inch by 4 inches in cross section with electrodes 18 inches long. The pulse length was 60 μsec. The transverse magnetic field was 2.35 webers/m^2. The total electrical energy delivered to the load in this case was 750 joules. The driving energy was derived from the detonation of 15 gms of RDX explosive in shaped charge geometry seeded on the front surface with 0.4 gms of cesium picrate. The conversion efficiency, chemical to electrical was 1%. Higher efficiencies can be readily obtained by using stronger magnetic fields and a longer generator. The time scale of the power pulse in the present experiments varied between 5 and 100 μsec depending upon the length of electrodes in the generator and the density of gas initially in the generator channel. Pulse lengths of between 1 and 200 μsec would be characteristic of practical systems based on the explosive driven MHD converter technique.

Extensive experimental and theoretical work has been performed on the explosive driven MHD generator concept to determine the basic physical processes occurring in the generator and to obtain the data necessary to scale the results to larger sized units with usable outputs. These investigations have covered: (1) the choice of explosive and explosive geometry, (2) the choice of pressure and composition of gases initially in the channel, (3) the selection of the optimum load and its proper placement across the electrodes, and (4) the effect of electrode geometry, magnetic field intensity, and the channel aspect ratio upon power output. The velocity, pressure, and conductivity of the detonation products was also determined.

From these studies it has been determined that highly conductive detonation products with a measured conductivity about 1100 mho/meter, are produced by seeding condensed explosives with a low ionization potential material such as cesium picrate. In the pulsed generator, the seeded detonation products pass at high velocity (10 km/sec) through an MHD channel which has a transverse magnetic field of up to 2.35 webers/m^2 so that the maximum induced voltage, u x B, is of the order of 200 volts/cm. The current is extracted by means of copper electrodes in contact with the detonation products and conducted to an external load. The detonation products are slowed as kinetic energy is converted to electrical energy and removed from the system.

On the basis of the experimental data presented herein it is now possible to predict the characteristics of explosive driven MHD generators with a fair degree of accuracy to meet a specified pulse requirement within the applicable time range.

2. Theory

The generation of pulsed power by MHD means from condensed explosives is a direct outgrowth of steady state experimentation and follows a somewhat parallel theoretical development. It

is instructive to recall that the electric power generated in an MHD generator feeding a resistive load is given by the relation

$$P = I^2 R_L = uBdI - I^2 R_i , \qquad (1)$$

where

P = power in watts,

u = velocity in meters per second,

B = magnetic field in webers per meter^2,

R_L = load resistance, ohms,

R_i = generator internal resistance, ohms, and

d = electrode separation, meters.

The generator internal resistance R_i is given as

$$R_i = \frac{d}{\sigma b a} \qquad (2)$$

where

σ = plasma conductivity, mho/m,

b = channel width, meters,

a = length of conductive region in axial direction, meters.

The maximum power is delivered to the load when $R_i = R_L$. It can be shown that in the low magnetic Reynolds number approximation, the maximum power output per unit volume is given as

$$\frac{P}{abd} = \frac{\sigma u^2 B^2}{4} . \qquad (3)$$

For the high pressures in the detonation product flow, the electron mean free path is small compared to the Larmor radius and therefore the Hall effect can be neglected.

Equation (3) implies that the magnetic Reynolds number is small and the current can increase without limit. However, at high magnetic Reynolds numbers where the magnetic Reynolds number is given as

$$R_M = \mu \sigma u L , \qquad (4)$$

where

μ = permeability,

σ = conductivity,

u = velocity, and

L = characteristic dimension which arises from the solution of Maxwells equations,

there is a maximum current which can be induced in the plasma. This current can be expressed as

$$I_{max} = \frac{2Bd}{\mu_o} , \qquad (5)$$

which would occur when driving low impedance loads.

In the explosive driven generator the velocities are 10^4 m/sec, and the conductivity is 10^3 mho/meter. Therefore, in a laboratory scale experiment with L = 0.04 meters,

$$R_M = 4\pi \times 10^{-7} \times 10^3 \times 10^4 \times 4 \times 10^{-2} = 0.5 .$$

We must therefore conclude that, in laboratory devices which are driven by condensed explosives, Equation (3) must be modified to some extent since Re_M is not much smaller than one. If large devices are considered, i.e., $L \sim 1$ meter, then

$$Re_M > 10 .$$

Equation (3) is definitely no longer valid, and the large Reynolds number expression must be used for power density. In Reference 3, this condition is shown to be given in the limiting case by the relation

$$P = \frac{2B^2}{\mu} Au , \qquad (6)$$

where $A = bd$ is the cross sectional area of the channel. For $Re_M \sim 1$ the power density will be between that given in Equations (3) and (6). Equation (6) arises from the fact that when $Re_M \gg 1$, the currents induced in the plasma conductor give rise to a magnetic field. This field is equal in magnitude to the initial field ahead of the moving conductor and in a direction such that the field value is doubled ahead of the conductor while the field behind the current sheet drops to zero. Thus, the braking pressure given by

$$P_z = \int (j \times B)_z \, dz$$

(where z is along the direction of motion) becomes

$$p = \frac{2B^2}{\mu} .$$

Therefore, the rate at which work is done is given by the product of this braking pressure and the rate at which volume is swept up, which is expressed as Equation (6).

It is interesting to notice that the power production for the case of $Re_M \gg 1$ is independent of σ and only depends on u to the first power. Thus, in large scale, pulse power devices it will not improve power output markedly to increase σ much beyond the point where $Re_M \sim 3$-4. It then becomes more important to maximize the velocity with which the conducting slug moves against the field, and to maximize the magnetic field. The removal of electrical energy from the system will, of course, slow down the detonation products. This effect has been experimentally observed.

3. Experimental Apparatus

The experimental apparatus used for the experiments consists of five basic parts as shown in the schematic in Figure 1. These are: (1) explosion chamber or driver section; (2) the MHD channel or test section; (3) diagnostic instrumentation; (4) electromagnet, and (5) evacuated dump tube and tank. Figure 2 is a photograph of the complete facility; Figure 3 is an "exploded view" of the 1 inch by 4 inch generator. The explosive driver, the black object in Figure 3 just below the explosion chamber, is a 7.5 gram,

commercial shaped charge jet perforator. The explosive in the jet perforator is generally a waxed RDX (cyclo-trimethylene-trinitramine) composition. The copper liner of the perforator is removed prior to firing the charge. Firing is initiated by an electric blasting cap which sets off the explosive primacord. The primacord serves as an explosive train to carry the detonation to the booster at the base of the RDX charge. The explosive is seeded with a low ionization potential compound (cesium picrate) in a fashion which is described in a subsequent section. The charge (or charges) is held in place in the explosion chamber by a polystyrene spacer which provides standoff of the condensed explosive from the metal walls.

The driver section, or MHD generator proper, shown in Figure 3 is a steel channel. The walls of this test section are 0.75 inch thick. The top and bottom spacer bars which hold the electrodes are of stainless steel; the channel sidewalls are made of soft magnetic steel. The purpose of soft steel is to reduce the width of the gap in the magnet. With a lower reluctance, a given power source can produce a higher magnetic field in the test section. The inside walls of the channel are insulated with fiber reinforced phenolic strips (micarta). The test section is fitted with copper electrodes which are flush with the inside walls as shown in Figure 3. In some experiments, continuous electrodes the length of the generator were used. In other experiments the electrodes were spaced on two inch centers down the channel. The electrodes were unheated copper, 1.0 inch wide, but of varying lengths in the flow direction. The space between the segmented electrodes is filled with phenolic strips to maintain a smooth contour. In addition to experiments in the 1 inch by 4 inch channel, an MHD channel of 1 inch by 1 inch (in the direction of u x B) was also studied. It was the purpose of the experiments in the two channels to study the effect of aspect ratio and scaling parameters.

Readout of data has been accomplished with Tektronix 551 dual-beam oscilloscopes equipped with Polaroid cameras. A small triggering electrode, situated at the explosion end of the test section, senses the u x B voltage developed by the detonation products and triggers the oscilloscope sweeps. Resistive loads are fastened across the electrode pairs on the outside of the channel as indicated schematically in Figure 1. The resistive loads pass through the slots milled into the outside of the side plates (shown in Figure 3) so as to provide a minimum inductance path.

The cylindrical dump tank and muffler at the left side of Figure 2 is evacuated by a vacuum pump. The exit from the test section into the tank is sealed with a mylar diaphragm which is ruptured by the pressure pulse. The dump tank is employed strictly in order to muffle the noise produced by the explosive charge. The channel can be evacuated by a separate vacuum system, and then filled to a low pressure with any gas to be studied such as air, argon, helium, etc.

In the power generation experiments, the primary emphasis was placed upon the measurement of the voltage and current in the external load. Because of inductive effects, the voltage drop V across the external load is the sum of the ohmic drop and an inductive drop, i.e.,

$$V = IR_L + L \frac{dI}{dt} , \qquad (7)$$

where I is the current, R_L is the load resistance, L the load inductance, and dI/dt is the time rate of change of the current. Therefore, during the early part of the pulse when the current is rising, the voltage drop is greater than IR_L and correspondingly when the current is falling the voltage drop will be less. Therefore, it is not possible to determine the current from the measured voltage drop across the load resistor unless dI/dt and L are also known. Since time rates of change of current as high as 10^9 amperes/sec were observed, a load inductance of 5×10^{-8} henries resulted in a 50 volt inductive signal.

The voltage across the load was measured by means of coaxial cables which were connected to the differential inputs of a Tektronix type CA preamplifier. The recorded signal was the algebraic sum of the signals from the two ends of the load resistor. The cables were terminated in their characteristic impedance to avoid reflections. The outer shields were not grounded at the input end. The measurement was carried out in this fashion so that the load could be floated with respect to ground potential. The recording oscilloscopes were grounded to the test section at only one point, through the coaxial cable to the trigger electrode, so that ground loops were avoided.

The current through the load was measured separately by an inductive pick-up technique. The basic principle is to sense the magnetic field caused by the current through the load circuit. In practice the time rate of change of the magnetic field, dB/dt is sensed as a voltage by a pick-up coil placed near the conductor and then integrated with respect to time. For a pick-up coil of N turns, each with a mean area of A, at an average distance of r from the conductor, the induced voltage signal is:

$$V_i = NAdB/dt = \frac{2 \times 10^{-7} NAdI/dt}{r} . \qquad (8)$$

The voltage signal V_i is then integrated electronically in an RC network to produce a signal proportional to the current. This system can be calibrated by determining the response to a known current, or by determining the electrical characteristics of the system including: (1) the mutual inductance between the pick-up coil and the circuit conducting the current to be measured, (2) the number of turns on the coil, and (3) the resistance and capacitance of the integrating network.

If a toroidal pick-up coil is used, the response is independent of the location of the current carrying conductor, provided that the toroid is uniformly wound and encircles the current carrying conductor. When using a toroidal coil the coefficient of coupling between

the conductor in which the current is being measured and the pick-up coil can be expressed as the ratio L/N where L is the inductance of the toroidal coil and N is the number of turns on the pick-up coil. The details of a typical coil and integrator are shown in Figure 4. To eliminate signals due to externally generated time varying magnetic fields, (when viewed from the above toroid appears as a one-turn coil) the toroid is wound so that the return lead provides a back turn. This turn, to a first approximation, cancels out any voltage signal induced in the toroid by magnetic fields whose source is external to the toroid.

4. Power Generation Experiments

Figure 5 is a typical oscilloscope trace of the current and voltage output of the 1 inch by 4 inch explosive driven MHD generator with 18 inch long continous electrodes. For this experiment the magnetic field was 2.35 w/m^2. The channel had previously been evacuated and was filled to an initial pressure of 10 mm Hg. The load resistor for this case had an initial resistance of 20.1 milliohms and the channel was powered with two shaped charges with a total explosive of 15 grams of RDX. Each charge was seeded with 20 mg of cesium picrate. The sweep speed of Figure 5 is 10 microseconds per centimeter. The upper trace, which shows the voltage, has a gain of 200 volts/cm, while the current, shown in the lower trace, is 10.7 kA/cm. The peak current, which occurs about 30 microseconds after the start of the trace is 30 kA. The peak voltage which occurs at a later time, i.e., about 45 microseconds, is 800 volts. The power output of the generator which is the product of the current and the voltage, is shown as a function of time in Figure 6. The peak power in this pulse is about 23 MW which continues for approximately 15 microseconds after the time of peak current. The total pulse length is 60 microseconds. The value of the load resistance, as determined from the voltage divided by the current, is also shown in Figure 6. It can be seen that the resistance increases as the load heats up. The energy delivered to the load, which can be calculated by summing the area under the power versus time curve in Figure 6, is 750 joules. For this experiment where two charges were used to drive the channel, the chemical energy in the 15 grams of RDX contained in the charges is approximately 75,000 joules. Therefore, the overall conversion efficiency of the system, chemical energy to electrical energy, is presently 1%. Higher conversion efficiencies can be obtained by: (a) increasing the magnetic field, (b) increasing the utilization of the explosive through appropriate changes in geometry, and (c) increasing the channel length since the gases are still highly conductive when they leave the generator, so that additional energy can be converted.

As an independent check of the energy delivered to the load, calorimetric calculations have been performed for the load resistor used with the 1 inch by 4 inch channel. The initial load resistance at 20°C for the pulse shown in Figure 6 was 0.020 ohms. As energy is dissipated in the load during the pulse, the load is heated and the resistance increases as noted, to a value of 0.035 ohms. From the increase in resistance, and the known temperature coefficient of resistivity, mass of the load, and the specific heat of the load material, the energy dissipated in the load can be calculated as 710 joules which agrees within 6% with the value calculated from the electrical measurements.

To investigate the effect of load resistance upon power output, the data from the shot shown in Figure 5 is plotted together with other data taken in the 1 inch by 4 inch generator as Figure 7. This figure gives power outputs as a function of load for three separate gases initially in the channel: air, argon, and helium at 10 mm Hg initial pressure. It is seen that the highest power output was obtained using helium with a load resistance of 20 milliohms. The limited data which is available, and shown in Figure 7, suggests that the optimum load resistance for the 1 inch by 4 inch channel is approximately 20 milliohms.

To examine the variation in optimum load resistance with generator size, the power output for the 1 inch by 1 inch generator is plotted as a function of load resistance in Figure 8. The data on which this figure is based is similar to the data which was shown in Figure 5 except that the voltage levels are somewhat lower because of the smaller electrode separation. Figure 8 shows that the maximum power output in the 1 inch by 1 inch channel was achieved with a load resistance of 5 milliohms. This data indicates that the optimum load for a channel should be about 5 milliohms per square unit of channel cross sectional area. The power output in the smaller channel was approximately a factor of two larger when argon was used as the filling gas. However, in the larger channel the superiority of argon and helium over air as a filling gas is not clear. Having seen that appreciable power outputs can be achieved, a number of experiments have been conducted to investigate the effect of various parameters in MHD generator operation in order to optimize the generator output. The following section discusses this experimental program in some detail.

5. Technical Studies

Inasmuch as an understanding of pulsed generators simultaneously covers several areas of technology, i.e., explosives, MHD power generation, shock waves, ionization in explosives, etc., it was necessary to conduct a rather extensive program to investigate the effects of the many parameters upon the output characteristics of the explosive driven MHD generator. Since the power output of the generator depends primarily upon the velocity of the working fluid, the conductivity of the working fluid, the strength of the magnetic field, and the characteristics of the electrical load; the major emphasis was placed upon an investigation of these parameters and their effect upon the electrical output of the generator. A number of subsidiary studies were conducted in support of this objective, including measurements of the pressure in the channel, studies of the effect of explosive geometry

variations, and studies of the optimum explosive composition. Certain of these studies are presented in the following sections:

Variation of Velocity with Initial Pressure

One of the important parameters in determining the output of the explosive driven MHD generator is the velocity of the conductive zone, inasmuch as the output power varies directly with velocity in the high magnetic Reynolds number case, and as the square of the velocity for low magnetic Reynolds numbers. In the initial experiments with the channel at atmospheric pressure, it was determined that the velocity of the conducting detonation products was approximately 6 km/sec. However, if the pressure initially in the flow channel was reduced, a higher velocity was observed. Therefore, a systematic investigation of the variation in velocity with initial pressure was conducted.

In these experiments, the velocity of propagation of the conducting detonation products was measured by determining the time of arrival of the front of the conducting region at various stations along a 1 inch by 1 inch channel. The timing pulses were generated by discharging capacitors across several of the electrode pairs in an auxiliary channel which was instrumented expressly for these measurements. Arrival of the conducting zone at the electrode pairs allowed the capacitor to discharge through the channel and produced a voltage pulse across a 100 ohm resistor placed in series with the capacitor. Figure 9 is an X-t diagram showing the time of arrival of the front at various stations along the channel for several values of initial channel pressure.

The consistency of the velocity data obtained on different shots is excellent, with a variation of only a few percent in an extended series. The velocity, as determined from the slope of the X-t curve near the origin, has an initial value of about 12.5 km/sec for an initial pressure of 0.1 mm Hg of air. Some attenuation can be noted with distance down the channel, particularly at the higher pressures. The data suggest that, in the region between atmospheric pressure and 100 mm Hg, the velocity of the front increases slowly as the pressure is reduced. For initial pressures below 100 mm Hg, the velocity increases much more rapidly. For 10 mm Hg, the pressure used in the majority of the experiments, the average velocity is 10 km/sec, with little attenuation along the channel. While higher velocities could have been achieved by evacuating the channel to lower initial pressures, it was difficult to reliably attain lower pressures after a number of shots in the apparatus because of deformation of the sealing surfaces and the 10 mm Hg initial pressure was chosen as the operating pressure. It should be noted that, for most of the shots in the 1 inch by 1 inch channel, mylar diaphragms were used at both ends of the channel, and only the channel proper was at the low pressure. The explosive was at atmospheric pressure in the 1 inch by 1 inch channel. However, for most of the experiments

in the 1 inch by 4 inch channel, the explosive chamber was also evacuated.

Of considerable interest has been the explanation of the variation in velocity with initial pressure. Four theoretical models were explored in some detail to determine a possible reason for the variation in velocity with initial channel pressure. These models were:

1. blast wave,
2. the fast jet,
3. the solid propellant driven shock tube, and
4. shock wave.

The details of these studies are contained in Reference 4 where it was found that none of these models could adequately explain the observed variation.

The blast wave model[5] predicted that the position of the front should vary with time as

$$t = \frac{2}{3} \frac{E}{\rho_o B}^{1/2} R^{3/2} , \qquad (9)$$

where E is the energy release, ρ_o the initial gas density and B a constant which depends upon the specific heat ratio of the shocked gas and the geometry of the shock wave. The atmospheric pressure data fits this relation quite well. However, at lower pressures, i.e., as ρ_o approached zero, the above relation does not fit the data.

The fast jet model[6] was patterned after the fast jets observed from the collapse of cylindrical liners of light metals by condensed explosives. The model was discarded when it was discovered that the same high velocities were obtained at low pressure when using flat faced charges instead of the cone shaped charge.

In the solid propellant driven shock theory[7], no variation with initial pressure was predicted. The data are obviously at variance with this theory, and it was accordingly rejected.

Considerable effort was expended in examining the applicability of the shock wave model. This theory predicts that if the conductivity were due to shock heating of the air and the cesium seed material, the conductivity would vary markedly as the initial pressure was changed inasmuch as the shock traveled faster, e.g., the shock Mach number increased. The shock wave theory predicts that for a constant driver gas pressure in the explosion chamber, the Mach number should vary approximately as the inverse square root of the initial pressure, as in the blast wave model. The shock wave model also predicted a variation in shock peak pressure with initial pressure. It was found that the shock wave model failed three experimental tests in that: (a) the variation in conductivity with initial pressure, or velocity, was much smaller than predicted, (b) the velocity did not vary as the inverse square root of the initial pressure, and (c) by the use of propane, which has a specific

heat ratio of $\gamma = 1.11$, instead of $\gamma = 1.4$ as for air, it was found that the velocities and conductivities were independent of the specific heat ratio of the gas initially in the channel in contradiction with the models which ascribed the conductivity to shock heating of the air initially in the channel.

Perhaps the best explanation of the observed variation of velocity with initial pressure can be derived from a discussion of the emergence of a detonation wave from the surface of a condensed explosive. It can be shown [8] that for the expansion of the detonation products into empty space the velocity of the gases, u, is given by a relation of the form

$$u = D - c_x + \left(\frac{2}{\gamma - 1}\right)c_x = D + 5.67\,c_x , \qquad (10)$$

where D is the detonation velocity, and c_x is the velocity of sound in the explosion products after they have expanded to the point where the isentropic relation is applicable. In most cases c_x is approximately 1 km/sec, and $\gamma = 1.3$, so that for RDX at a density of 1.7 gm/cm^3, where D is approximately 8 km/sec, the maximum velocity should be about 13.5 km/sec for one dimensional expansion into empty space, which is in reasonable agreement with the value of 12.7 km/sec which was observed.

For completeness we will consider the case where the explosive is expanding into air and a shock wave is formed ahead of the detonation products. We will let the pressure in the air shock be equal to p. The pressure in the detonation products will be reduced to this value by expansion. We will assume that for the strong shock in air, $\gamma = 1$ so the velocity of the shock u is given as

$$u = \left(\frac{p}{\rho_c}\right)^{1/2} , \qquad (11)$$

where ρ_c is the initial air density. The velocity u should be equal to the velocity of the explosion product in the rarefaction wave, as given above, but modified by the fact that the velocity of sound in the explosion products is also reduced. Equating the velocity at the interface between the explosion products and the thin layer of shocked air we obtain

$$u = \sqrt{\frac{p}{\rho_o}} = D - c_x + \frac{2}{\gamma - 1}\,c_x\left[1 - \frac{p}{p_x}\right]^{\frac{\gamma - 1}{2}} . \quad (12)$$

For a typical explosive, p_x, is approximately 4000 atmospheres. In air at atmospheric density, $\rho_o = 1.3 \times 10^{-3}$ gm/cm^3. Substituting these values we can solve Equation (12) by numerical methods to find that the pressure in the air wave, p, is approximately 1/10 of p_x, or 400 atmospheres, and the particle v   , is approximately the detonation vel

The above model is in excellent agreement with the observed data when it is considered that the measured velocity is determined by the transit time between two stations and is therefore an average velocity, whereas the initial velocity is much higher, near the detonation velocity as predicted.

The important feature of this theory is that there is a maximum limiting velocity as the initial gas density is reduced in agreement with the experimental data. The highest velocities are obtained when using an explosive with a high detonation velocity, D, and when expanding into a vacuum. If ambient gases are present, i.e., air or argon as in the experiments reported herein, the velocity will be reduced by a factor which is dependent upon both the isentropic properties of the explosive and the shock properties of the ambient gases. However, because of the ionization which might occur in the ambient gases due to strong shock, there is the possibility that the maximum power production conditions will occur at some optimum pressure where the product u σ is maximized, and not at the highest particle velocity u, which would occur if the charge were exploded in vacuo.

Seeding Studies

In the early experiments it was quickly noted that seeding of the explosive with a low ionization potential material was required in order to produce appreciable amounts of power, i.e., obtain high electrical conductivity. In a typical set of experiments in the 1 inch by 1 inch channel with a magnetic field strength of 1.5 w/m^2 and with the channel initially at atmospheric pressure, an unseeded 7.5 gm charge gave an open circuit voltage of 130 volts. The generator had an approximate internal resistance of 150 ohms as determined from the voltage-current plot. The maximum power delivered to the load was about 28 watts. When an identical 7.5 gm charge was seeded on the surface with 0.2 gms of cesium carbonate, the open circuit voltage rose to 230 volts, the internal impedance dropped to 0.5 ohms, and the power to the load increased to 74 kW. These data indicate that the internal impedance decreased by a factor of 300, i.e., the conductivity increased by a similar factor. Experiments were then conducted with an active seed material, i.e., one that liberates energy. Cesium picrate was selected as the most satisfactory from many consideration. With 0.2 gms of cesium picrate seed on the surface of the 7.5 gm charges and identical channel conditions, another factor of five was obtained in power output over the value obtained with cesium carbonate. Figure 10 shows the results of a set of experiments undertaken to show clearly the effect of using cesium picrate seed material. Figure 10 is a voltage-current plot of data taken under identical conditions using seeded and unseeded charges. The seed was 200 mg

of cesium picrate placed on the inside surface of the cone of the charge. The data is of significance in that each point corresponding to a common load resistance was taken without disconnecting the load and in immediate time sequence. The difference in internal impedance between these two series of experiments was approximately a factor of 70. Note that the data of Figure 10 are plotted in semilog fashion because of the wide range of currents covered. These results clearly establish the desirability of seeding the explosive with low ionization potential materials.

To determine the optimum seed level for charges used to drive the 1 inch by 4 inch channel, a series of experiments were conducted where the channel was evacuated and then filled with 10 mm Hg of argon. Different amounts of seed were used for each shot. The results of these experiments are shown in Table 1 which lists the peak current through a 20 milliohm load resistor as a function of the mass of cesium picrate used on each of two explosive charges. Also given in Table 1 are the peak voltages (which may not occur simultaneously with the peak current) and the length of the pulse, as determined by the time to the sharp cut off in the voltage trace. It can be seen that the peak current, and hence highest power output, occurs for the 200 mg seeding case (e.g., 200 mg seed on each of two driving charges). The pulse is lengthened as the amount of seed is increased. It should be noted that considerable power can be drawn even if no cesium picrate is used, i.e., the argon is shock ionized and acts as the conductor. This is similar to earlier experiments where MHD power was drawn from the shock waves, i.e., the work of Nagamatsu[9] in air, and Pain and Smy[ ] in argon. In the present experiments, it should be noted that the maximum power is generated when both argon and cesium picrate are used.

Table 1

Effect of Seed Level on Output in the 1 Inch by 4 Inch Generator

Seed mg/charge	Peak Current, kA	Peak Voltage, volts	Pulse Length μsec
0	17.7	380	45
50	24.1	550	44
100	26.8	660	49
200	28.0	710	47
300	26.8	660	49
400	27.8	680	49

In summary the choice of the optimum seed system is rather complex and will depend upon many factors. In particular it appears as though, once the conductivity is high enough so that the magnetic Reynolds number approaches unity, the output becomes independent of the conductivity, and other factors such as the effect of the seeding system on the detonation product velocity become important in controlling the output.

Conductivity Measurements

Because the electrical conductivity σ is a sensitive function of the temperature of the electrons in the conducting gases, information regarding the variation of conductivity with initial channel gas density should help explain the mechanisms responsible for the conductivity. Also, the conductivity data, per se, is important for the power generation experiments since, it determines the magnetic Reynolds number, R_M, for a fixed velocity. The power output characteristic is a function of R_M as has been previously outlined. The conductivity is also one of the most difficult parameters to measure.

In the power generation experiments it was possible to make a determination of the plasma current the internal voltage drop, and the size of the conductive slug from which the conductivity can be determined. These experiments were conducted in the 1 inch by 1 inch channel with an initial pressure of either 10 or 760 mm Hg of air, in the channel. The magnetic field was 1.7 w/m², and the standard explosive charge with 200 mg of cesium picrate was used as a driver. In the majority of the experimental shots the electrode length was 2.0 inches.

Figure 11 is a typical oscilloscope trace showing the current and voltage across a 9.45 milliohm load resistor. The sweep speed is 2 microseconds per centimeter, the voltage gain is 50 volts per cm (upper trace), while the gain for the current (lower trace) is 1070 amperes/cm. The peak current, shown in the lower trace, is 3500 amperes, which would indicate a power generation level of approximately 115 kW at the time of peak current. The power pulse lasts for about 6 microseconds, then falls off rapidly, with a dI/dt of about 10^7 amperes/sec. During the time the current is falling the voltage trace goes negative showing the inductive effect to be much larger than the ohmic voltage drop. From the measured dI/dt and the measured voltage drops, it is estimated that the inductance of the external load is 0.07 μh. Thus, despite efforts to maintain the load inductance as low as possible, the current is inductance limited over part of the range of the experiment. In this case the conductance of the plasma column can be determined from the data taken at the peak current when dI/dt = 0, so that the internal voltage drop can be determined from the relation

$$IR_i = Bd - IR_L .$$

The peak current and voltage data from a large number of shots similar to the one shown in Figure 11, but with different load resistors, are plotted in Figure 12. Also shown in Figure 12 are a limited number of data points for shots where the initial channel pressure was atmospheric. The solid lines through the points represent the generator voltage-current characteristic, or load line, for the two initial pressures. The generator internal resistance or conductance is determined by the slope of the voltage-current characteristic curve. If the dimensions of the current carrying channel are known, and a uniform electric field can be assumed, the conductivity can be calculated from the conductance.

The similarity in slope between the two characteristics, i.e., 0.109 ohms for the atmospheric pressure curve, and 0.0717 ohms for the 10 mm Hg curve, indicates that the conductivity is practically independent of the initial channel pressure and hence is independent of the Mach number.

From a similar series of experiments using 1/2 inch diameter round electrodes it was determined that the internal resistance of the generator was 0.08 ohms, or only a factor of 1.1 higher than for the 1 inch by 2 inch electrodes. Since the electrode area differs by a factor of 10, it is assumed that the small difference in internal resistance results because the area occupied by the highly conducting detonation products is small compared to the size of the large electrodes. This view is supported by an examination of pulse length versus electrode length. The velocity of the gas is roughly 10 km/sec or 1 cm/microsecond. Therefore, the transit time for a 2 inch electrode would be 5 μsec. It can be seen in Figure 12 that the current maximum occurs at about 6 microseconds, which would indicate that the conductive slug is of the order of 1 cm long.

Data on pulse length was also taken using electrodes of the following lengths: 2.0 inches, 1.0 inch, and 0.5 inch. Extrapolating this data to zero electrode length gave a pulse length of 1.5 microseconds which would correspond to a thickness of 1.5 cm for the conductive slug in good agreement with the above. Under the assumption that the conductive material uniformly fills a 1.5 cm length of the flow channel, and that the electrode length is long compared to the thickness of the slug so that electrode fringing factors need not be considered, the conductivity of the channel is 1000 mhos/meter. If an allowance is made for the 40 volt electrode drops which are indicated by probe measurements, the conductivity of the seeded detonation products is 1100 mho/meter. This conductivity, in a direction perpendicular to a strong magnetic field would correspond to a plasma temperature of 9000°K, using the Spitzer relation [10],

$$\sigma = \frac{7.75 \times 10^{-3} \, T^{3/2}}{Z \ln \Lambda} \ (\text{mho/m}), \qquad (13)$$

where it is assumed that the product of the ionic charge, Z, times the logarithm of the Debye cut-off parameter, Λ, has the numerical value of 6. The reason for the high apparent temperature is not known. However, it may be implied that most of the cesium is ionized.

In the power generation experiments, the ionized detonation products are conductive at least for times up to 30 microseconds. However, as will be discussed in the following section the voltage-current relation is very non-linear when long electrodes are used, whereas, for the experiment with short electrodes reported in this section, the voltage-current characteristic curve is reasonably linear. The

reason for the non-linearity is not known. The present evidence supports the view that the non-linear characteristic is due to both internal joule heating [11] and due to an increase in the axial dimension of the conductive slug.

In summary, it may be stated that very high conductivities are observed in the seeded detonation products and the conductivity exists for times sufficiently long that an appreciable fraction of the kinetic energy of the detonation products can be converted to electrical energy.

Variation in Output with Load Resistance

Important information can be gained by examining the output of the explosive driven MHD generator as the load is changed from open circuit conditions, to short circuit. In the normal MHD generator theory, the open circuit voltage is given by the relation

$$V_o = uBd, \qquad (14)$$

where u is the gas velocity, B is the magnetic field strength, and d is the separation between electrodes. If the electrodes are connected to an external load so that currents can be drawn through the generator, then the voltage across the load will be given by

$$V = V_o - IR_i = IR_L, \qquad (15)$$

where I is the current through the generator, R_i is the internal impedance of the generator and R_L is the load impedance. In the more general case, which must be considered here because of the short pulse length, inductive effects must be included. Under these conditions we have

$$V = IR_L + L_L \frac{dI}{dt} = V_o - IR_i - \frac{d}{dt}(L_i I)$$

$$= V_o - IR_i - I \frac{dL_i}{dt} - L_i \frac{dI}{dt}, \qquad (16)$$

where L_L and L_i are the inductances of the load and the internal inductance of the generator, respectively. By variation of R_L and L_L, the external parameters most readily available for change, and by measuring I and V, it is possible to estimate R_i and L_i, if it can be assumed that V_o is constant over the change in parameters. From Figure 9 it is seen that u is not constant along the channel and, furthermore, as will be noted later, it is possible to slow the gases down by approximately 10%, by the extraction of energy with low values for the load resistance. However, as a first approximation it will be assumed that V_o is constant. If the measurements are made at the peak current, then $dI/dt = 0$, and this relation simplifies to

$$V = IR_L = V_o - I_m \frac{dL_i}{dt} - I_m R_i, \qquad (17)$$

where I_m is the peak current.

By plotting V as a function of I_m, then one can evaluate R_i and dL_i/dt, assuming the R_i does not vary with the current level. Figure 13 is a

voltage-current plot of the V and I_m data taken in the 1 inch by 1 inch test section, using the 16-inch long continuous electrodes, and with the channel initially filled with 10 mm Hg of air. The first thing which is evident is that the voltage current relation is non-linear. The initial slope, at low currents, corresponds to an internal resistance R_i of 70 milliohms, which is in agreement with the short electrode data shown in Figure 12. As the current level increases the curve flattens out, with internal resistance approaching 5 milliohms in the range between 10 and 20 kA. Because of the wide range of currents which are covered in these experiments, it is better to plot the data on semilog paper as is shown in Figure 14. In this plot, lines of constant resistance have a characteristic shape but they are not straight as in the linear plot. One thing which becomes more readily apparent in this plot is the value of the short circuited current which is estimated as 25 kA. Also shown on Figure 14 are dotted lines which show the expected variation in V with I assuming a constant internal impedance R_i, and $dL/dt = 0$ with V_o assumed equal to 340 volts. It can be seen that the apparent internal impedance decreases with increasing current. Making the additional assumption that R_i is equal to 70 milliohms, as is indicated by the low current data, it is then possible to quite accurately fit the data with the relation

$$V = 340 - 0.07 I_m + 8 \times 10^{-6} I_m^2 , \quad (18)$$

where I_m is in amperes and V is in volts. Presumably the last term in the above equation represents such factors as the time changing inductance terms, which could include magnetic bootstrapping effects, and non-linear conductivity which appears similar to the transition to an arc mode which would have a negative resistance characteristic.

Also drawn as dashed lines on Figure 14 are lines showing constant power output. The peak power in these experiments with the 1 inch by 1 inch channel using air at 10 mm Hg as the filling gas was about 1.3 MW.

The data for the argon experiments are shown in Figure 15. The details of these experiments were identical to those reported above except that the channel was evacuated and then filled to a pressure of 10 mm Hg with argon. The results of the two experiments are similar except that the peak current is about a factor of two higher for the argon experiment. The peak power in the argon runs was about 3 MW. As before, it is possible to fit the data with a series expansion in the current variable of the following form:

$$V = V_o - IR_i + \beta I^2 = 325 - 0.015 I + 3 \times 10^{-7} I^2, \quad (19)$$

where β is the second coefficient of the expansion. Comparison with the data for air shows that V_o is only slightly lower than for air, whereas R_i with argon is a factor of 5 lower, and β is a factor of 25 lower.

The lower value for V_o is consistent with a decrease in velocity which was observed when the initial pressure of argon is increased, and represents the difference in mass of the comparable volumes of air or argon which are swept up by the detonation product front moving down the channel. The reasons for the change in R_i and β are more subtle. Measurements were made of the characteristics of the generator for experiments where the channel was maintained at 10 mm Hg of argon, but no seed was used in the explosive charge. In one experiment where a 6 milliohm load resistor was used, a current of 9.2 kA was measured, as compared to the 20 kA current shown in Figure 15. This experiment implies that the argon is ionized by the explosive shock and is capable of achieving high levels of conductivity, of the order of 700 to 1000 mho/meter, which is comparable to the conductivity of the detonation products. Thus, there can be two possible paths for the generator current, i.e., through the ionized cesium in the detonation products and through the ionized argon. The increase in current when using both cesium seed and argon accounts for the increase in output power shown in Figure 8.

Variation in Output with Magnetic Field

The output voltage of an MHD generator is a function of the applied magnetic field, i.e.,

$$V = uBd - IR_i - \frac{d}{dt}(L_i I) . \quad (20)$$

Therefore, if we make a measurement of the open circuit voltage, where $I = 0$ we can examine the effect of the magnetic field upon the output of the generator by comparing the data to the relation

$$V_{oc} = uBd, \quad (21)$$

where u, B and d are measured separately and independently.

Figure 16 is a plot of the open circuit voltage of the 1 inch by 1 inch generator when it is operated with the channel initially at atmospheric pressure as a function of the applied magnetic field. Equation (21) fits the data very well. The effective velocity u as derived from the slope of Figure 16 is 1.7 km/sec, whereas the measured velocity of the propagation of the front of the conductive region is 6.0 km/sec. One possible explanation for this descrepancy is that the velocity of the gas behind a shock is equal to the shock velocity minus the velocity of sound in the shocked gases or detonation products, i.e.,

$$u = M a_o - c_x , \quad (22)$$

where M is the Mach number, a_o the speed of sound in air, or the gas in which the shock is propagating, and c_x is the velocity of sound in the detonation products. This data would suggest that c_x is 1.3 km/sec.

The data from the power generation and conductivity experiments which were conducted at lower pressures do not agree as well with Equations (21) and (22). For example, the data expressed by Equation (18) gives the measured

effective product uBd of 340 volts. For an electrode separation of 2.54 cm, and a magnetic field of 1.7 w/m^2, the effective velocity is u = 7.9 km/sec, whereas the measured velocity is 10.3 km/sec. The limited open circuit voltage data taken with the 1 inch by 4 inch generator indicate the same sort of discrepancy. The data suggest that the output voltage is a constant fraction of about 0.8 of the uBd product. On this basis it is indicated that the problem is not due to electrode drops, or sheaths, etc., which would tend to be a smaller fraction of the open circuit output in the larger generator, but is due to some other factor.

One possible explanation is that the effect is due to circulating currents which arise because of the axial velocity distribution of the detonation products. The back and the front of the conductive slug, which move at different velocities, are connected by the electrodes which provide an axial path for the circulating currents.

Load Placement Studies

During the course of the experimental program it was discovered that under some conditions the output of the generator depended upon the physical location of the load. If the load was connected at the downstream end of the long electrodes, currents flowing through the electrodes changed the magnetic field in front of the conductive slug by "magnetic bootstrapping." For the 1 inch by 1 inch generator feeding a 1.3 milliohm load the current was increased by a factor of two, from 6.85 kA to 15.0 kA, when the load resistor was moved from the upstream end of the electrode to the downstream location. To explain this effect the following theory, which views the generator in terms of lumped electrical parameters, was developed.

Inasmuch as the generator electrodes are extended and may therefore contribute appreciably to the impedance of the generator-load circuit, the question arises as to the most favorable position for the local connection of the load. As the plasma conductor moves from one end of the electrodes to the other, the inductance and resistance of the circuit may vary appreciably in time. Clearly the functional character of the variations depends on whether the load is connected to the upstream end of the electrodes, to the downstream end, or perhaps to some intermediate point.

Some insight into this question of load position is readily derived from the following simplified lumped-parameter description of the circuit. Let L and R be the total inductance and resistance of the circuit consiting of the moving plasma conductor, electrodes, leads, and load. Let u be the speed of the plasma

conductor and B the magnitude of the applied field through which it moves. Neglecting displacement currents the Kirchhoff equation for the circuital current I is

$$\frac{d}{dt}(L\,I) + R\,I = uBd\,s(t) , \qquad (23)$$

where d is the interelectrode spacing and s(t) is a unit step function in time taking t = 0 as the time the plasma conductor first bridges the electrodes.

In general, u, B, L, and R are time dependent. The parameters L and R depend explicitly on the position of the load. For simplicity in the present analysis let the resistance be considered essentially constant, R_o say.

If now the inductance is expanded in a power series of a suitable expansion parameter, α, the current can be similarly expanded:

$$L(t, x) = L_o + \alpha L_1(t, x) + \dots \qquad (24)$$

and

$$I(t, x) = I_o(t) + \alpha I_1(t, x) + \dots \qquad (25)$$

where x is the position of the load connections from the upstream end of the electrodes. Substituting into (23) yields the following equations for I_o and I_1

$$L_o\,\frac{dI_o}{dt} + R_o I_o = uBd\,s(t) \qquad (26)$$

$$L_o\,\frac{dI_1}{dt} + R_o I_1 = -I_o\,\frac{dL_1}{dt} - L_1\,\frac{dI_o}{dt} . \qquad (27)$$

It is to be noted that the right hand side of Equation (27) for I_1 contains a source term proportional to I_o and is positive when the inductance decreases with time. This term accounts for the voltage induced in the plasma conductor as it moves through the magnetic field arising from the current I_o.

If it is assumed that u and B are substantially constant, the solution of (26) is simply

$$I_o(t) = \frac{uBd}{R_o}(1 - e^{-t/\tau}),\ 0 \le t \le \ell/u , \qquad (28)$$

where the current rise time is $\tau \cong L_o/R_o$ and ℓ is the length of the electrodes.

The solution of (27) is, after partial integration,

$$I_1(t, x) = -\frac{L_1(t, x)}{L_o} I_o(t)$$

$$+ \frac{e^{-t/\tau}}{\tau} \int_0^t e^{-t/\tau}\,\frac{L_1(t, x)}{L_o}I_o(t)\,dt. \qquad (29)$$

Given the functional dependence of L_1 on time and the position of the load connections the current can be determined.

The average power delivered to a load resistance R_L is evidently

$$\bar{P} = \frac{u}{\ell} \int_0^{\ell/v} I^2(t, x) R_L \, dt. \quad (30)$$

An extreme in the average power occurs when the load is positioned at x as given by $\partial \bar{P}/\partial x = 0$, or

$$\int_0^{\ell/u} I(t, x) \, \frac{\partial I(t, x)}{\partial x} \, dt = 0. \quad (31)$$

As a particularly simple example of the effect of varying the position of the load, consider the limiting case for which the current rise time is long compared with the transit time of the plasma conductor along the electrodes. According to (25), (27), and (28) then

$$I(t, x) \approx I_o(t) - \alpha \, \frac{L_1(t, x)}{L_o} \, I_o(t), \quad \tau > \ell/u. \quad (32)$$

Substitution of the current given by (32) into condition (31) yields

$$\int_0^{\ell/u} I_o^2 \, \frac{\partial L_1(x-ut)}{\partial t} \, dt = 0, \quad (33)$$

when terms to first order in α are retained in $\bar{P}$. It is assumed that L_1 is a function of the distance between the plasma conductor and the load connections. For definiteness consider a primitive bilinear function, namely

$$L_1(x-ut) + L_o \left| \frac{x - ut}{\ell} \right| . \quad (34)$$

According to (33) then the condition for a maximum in load power occurs when the load connections are at a distance x from the upstream end of the electrodes as given by

$$\int_0^{x/u} I^2(t) \, dt = \int_{x/u}^{\ell/u} I_o^2(t) \, dt. \quad (35)$$

Thus, it is found that in the case for which $\tau = L_o/R_o \gg \ell/u$ the load connections should be made at point along the electrodes on either side of which the areas under $I_o^2(t)$ are equal.

In addition to consideration of load position there is the question of the load impedance for maximum power transfer. The usual statement of the power-transfer theorem is that the load impedance should be the complex conjugate of the generator impedance; that is, a negative inductance should be inserted in series with the load. Crudely applied to the present

model, the theorem would require that a capacitor on the order of

$$C \sim \frac{4L_o}{R_o^2} \quad (36)$$

should parallel a load resistance equal to the internal resistance of the generator.

In conclusion, it is perhaps noteworthy that Equation (23) admits an integrating factor $\exp \int \frac{R}{L} \, dt$ which leads readily to the general solution

$$I(t) = \frac{d}{L} \, e^{-\int \frac{R}{L} \, dt} \int_0^t uBe^{\int \frac{R}{L} \, dt} \, dt, \quad 0 \leq t \leq \ell/u. \quad (37)$$

The above solution for the current by successive approximations is practically useful only if the time-variant contribution by the electrodes to the total inductance is relatively small. Solution (37) is, of course, not restricted by this condition and may be useful for more detailed analytical investigations. It should be appreciated that in reality R, B, and u as well as L will be time varying. If these parameters can be experimentally determined, numerical methods can be used to determine the optimum position of the load.

Probe Studies

When using a long, continuous electrode in the explosive driven MHD channel, it is difficult to determine the position and hence the velocity of the conducting front. To determine this information and to estimate the length of the conducting region, a series of four probes was installed in the upper electrode. The four probes were copper wires 1.5 mm in diameter, installed in holes drilled through the four electrode mounting studs. The probes were insulated from the electrode structure and were flush with the surface of the electrode in contact with the gas stream. They were mounted at distances of 4.5, 14.6, 24.7, and 40.0 cm respectively from the trigger electrode. For these experiments, which were conducted in the 1 inch by 1 inch channel, the magnetic field was 1.7 w/m^2 and the initial pressure was 10 mm Hg of either air or argon. Figure 17 is a composite drawing which shows the four probe traces plotted with their origins at the appropriate distance along the channel in the form of an X-t diagram. It can be seen that the detonation products propagate in air with a sharply defined front. It is also apparent that the slug of detonation products has a structure that expands as it flows down the channel and would cause a distribution in velocities along the conducting slug. There is a sharp spike in the traces for the third and fourth probes at about 46 microseconds, apparently caused when the rear of the conducting slug leaves the electrode.

It can be seen that the velocity is attenuated slightly as the detonation products move down the channel. The initial velocity is approximately 12.1 km/sec, which slows down to 8.9 km/sec between the third and fourth probes. The average velocity is 10.3 km/sec over the length of the channel with this load. For this experiment the load resistance was 19 milliohms and the total energy output was 43 joules. An average of data taken with an 0.5 ohm load resistor, which is almost equivalent to an open circuit condition, indicates an average velocity of 10.5 km/sec. These results would imply that the removal of 43 joules of energy has slowed the detonation products by 0.2 km/sec.

A number of similar shots were made with argon as the initial gas in the channel. In the argon shots there is a precursor which causes the voltage on the probe to rise before the front arrives. It is generally possible to determine the arrival of the front by a steep increase in voltage on the probe. From data taken with various load resis _s, it was possible to calculate the energy output for each shot and to measure the slowing down from the time required for the front to reach the fourth probe. Several shots were taken with each load resistor so that there is some degree of confidence in the results.

Figure 13 is a plot showing the change in velocity as a function of the number of joules delivered to the external load. It can be seen from Figure 18 that removing 16.5 joules of electrical energy slows the detonation product front by 0.1 km/sec. This data supports the previous assumption that the velocity was not markedly changed in the present experiments by the MHD interaction. The fact that the detonation products are appreciably slowed by the removal of this amount of energy indicates that the actual conversion efficiency, mechanical to electrical, is almost an order of magnitude higher than the indicated chemical to electrical conversion efficiency.

6. Conclusion

It has been demonstrated that short pulses of electrical power can be generated by MHD principles using condensed explosives as the energy source. This work has been particularly successful in that large pulses of power have been obtained with relatively high conversion efficiencies. The scaling of these results to larger sizes to produce systems with greater outputs appears relatively straightforward. Additional work is needed to determine the optimum values for the various parameters, however, the basic principles are well understood and the direction for future work to increase output and efficiency can be clearly outlined.

7. Acknowledgments

The authors would like to acknowledge the invaluable contributions of Dr. Paul Thiene, Dr. Peter Smy, Dr. Robert Brumfield, Mr. Earl Evans, and Mr. J. Tom Naff.
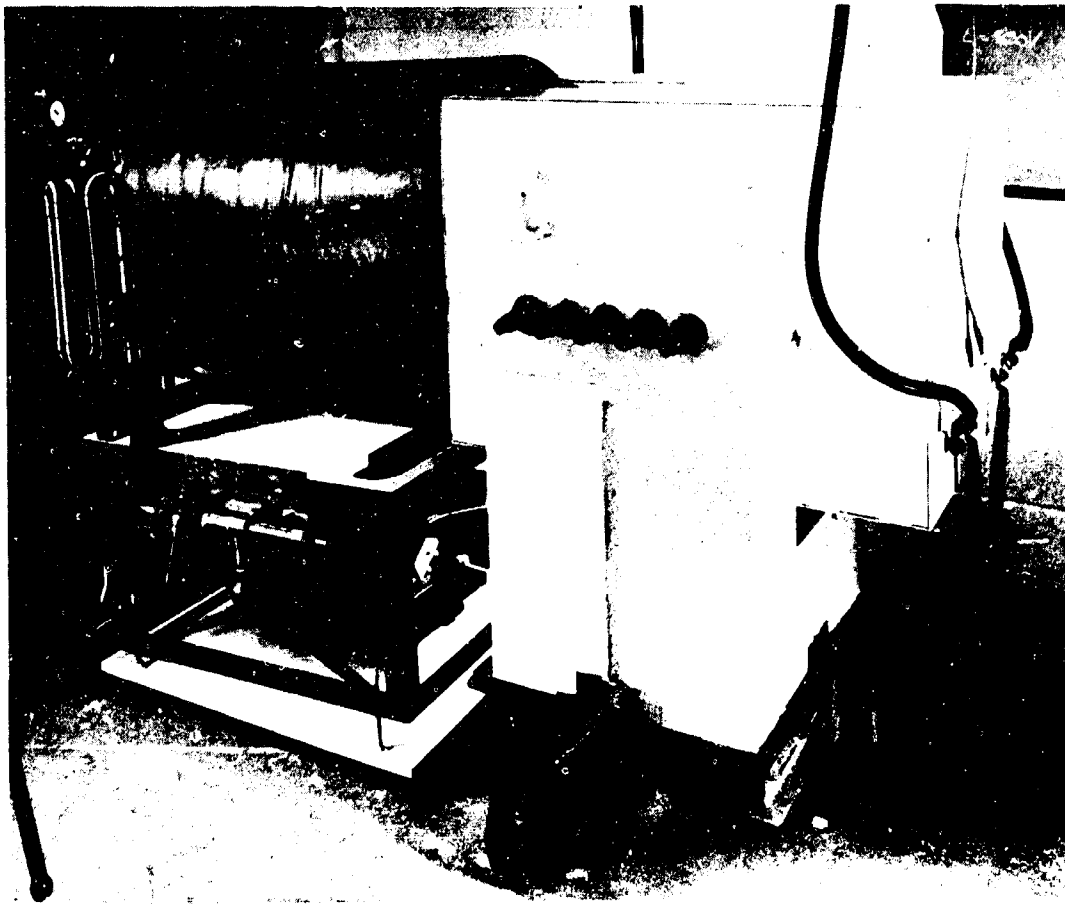
8. References

1. Brumfield, R. C., Evans, E. W., and McKinnon, C. N., Pulsed MHD Power Generation, Fourth Symposium on Engineering Aspects of MHD, Berkeley, California, April 1963.

2. Jones, Malcolm S., Jr., Blackman, V. H., Brumfield, R. C., Evans, E. W., McKinnon, C. N., Research on the Physics of Pulsed MHD Generators, MHD Research, Inc. Final Report No. 646, Dec. 1963.

3. Pain, H. J., and Smy, P. R., J.F.M., 11, 51, Feb. 1961.

4. Jones, Malcolm S., Jr., et al, Research on the Physics of Continuous and Pulsed MHD Generators, Second Semiannual Technical Report, MHD Research, Inc., Report 640, August 1963.

5. Jones, D. L., The Energy Parameter B for Strong Blast Waves, National Bureau of Standards, Technical Note 155, July 1962.

6. Koski, W. S., Lucy, F. A., Shreffler, R. G., and Willig, F. J., Phys. Fluids 23, 1300, Dec. 1962.

7. Rosciszewski, Jan, ARS Journal, p 1462, Sept. 1962.

8. Zeldovich, Ia. B., and Kompaneets, A. S., Theory of Detonation, Academic Press, New York and London, 1960.

9. Nagamutsu, H. T., Sheer, R. E., and Weil, J. A., Non-Linear Electrical Conductivity of Plasma for Magneto-hydrodynamic Power Generation, ARS Paper 2632-62, Space Power Systems Conference, Santa Monica, California, Sept. 1962.

10. Spitzer, L. J., Physics of Fully Ionized Gases, Interscience Publishers, New York, 1956.

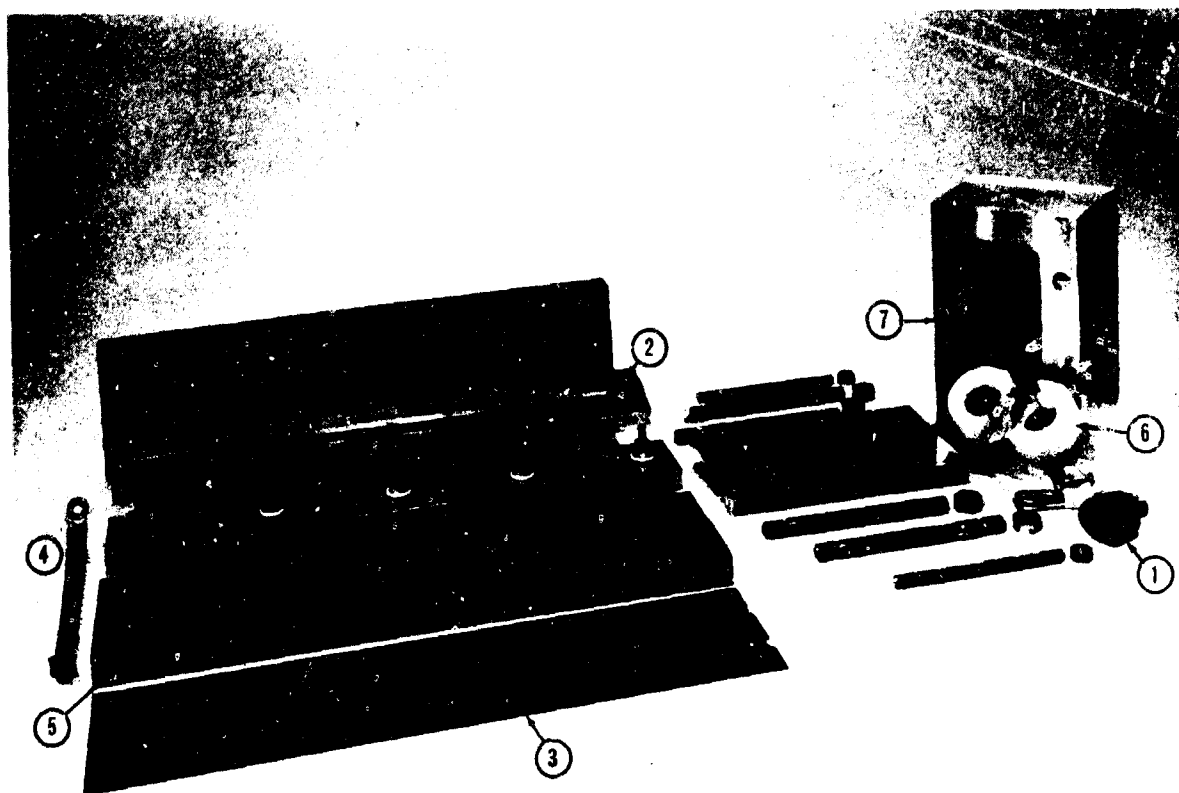11. Rosciszewski, Jan, and Oppenheim, A. K., Phys. Fluids 6, 689, 1963.

Labels on figure:

- Explosion Tube
- Blasting Cap
- Shaped Charges
- Electrodes
- Field Vectors
- Primacord
- Load Resistance
- Magnet Pole Face
- Mylar Diaphragm
- Dump Tank

Field vector labels: v, B, u
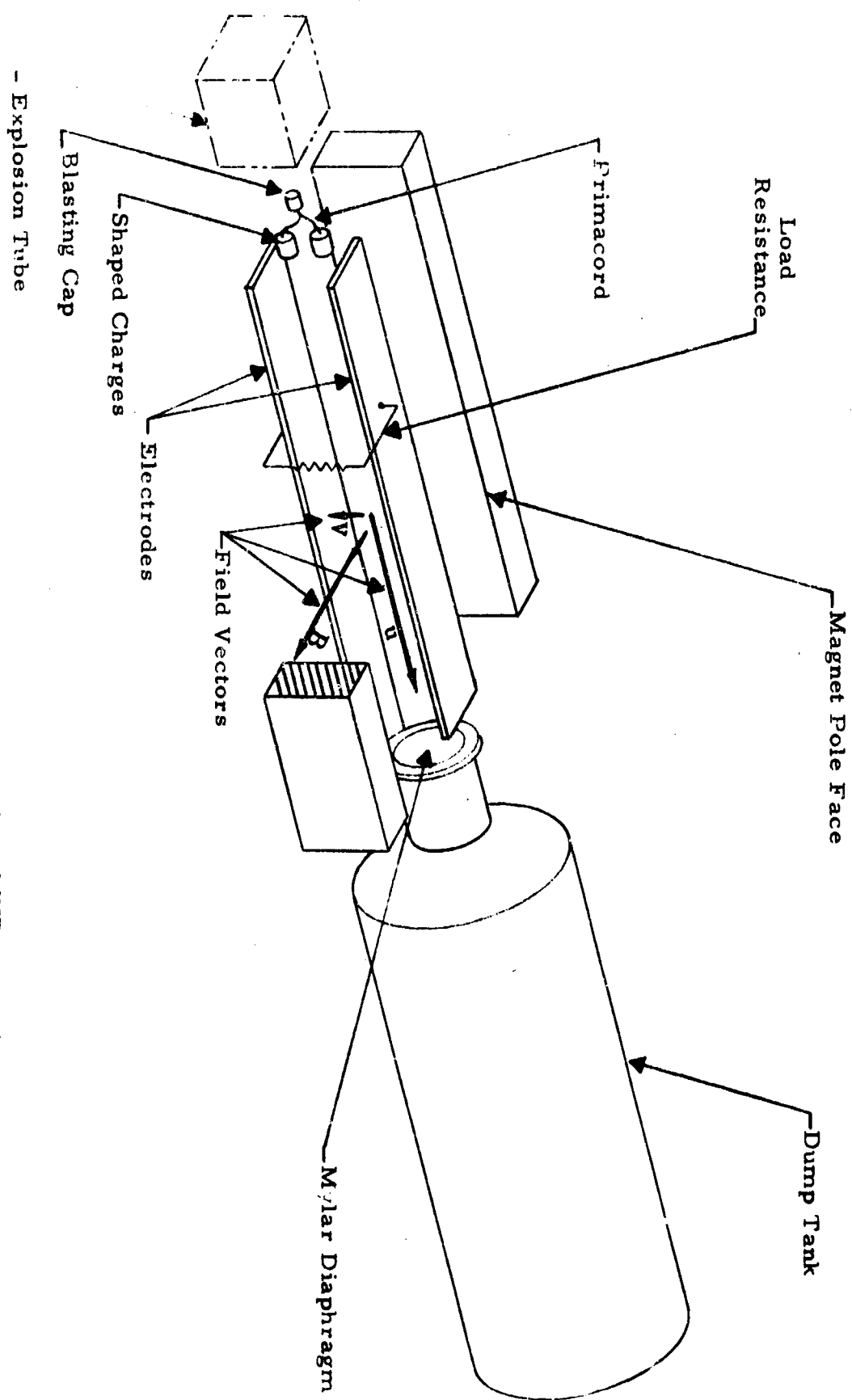
Schematic view of explosive-driven MHD generator.

Figure 1

View of complete facility

Figure

1. Shaped charge
2. 18" x 1" electrode
3. Bakelite sidewalls liner
4. Generator load
5. Slot for exterior surface of sidewall for resistive load
6. Standoff spacer
7. Explosion chamber

Figure

Dissembled view of 1" x 4" explosive driven MHD channel
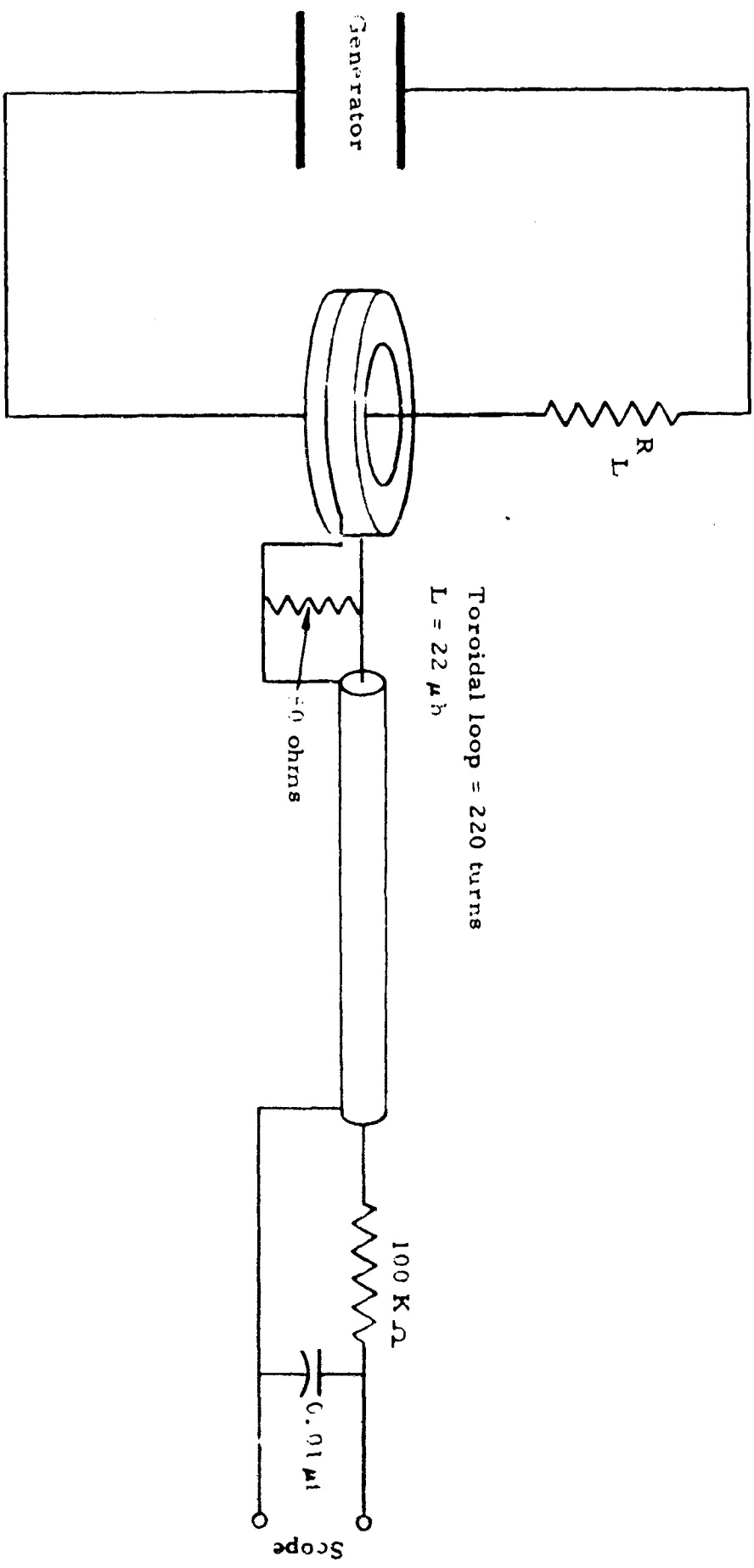
Figure 4

Schematic diagram of the current pickup loop and integrator circuit.
This circuit allows for an independent measurement of the current.
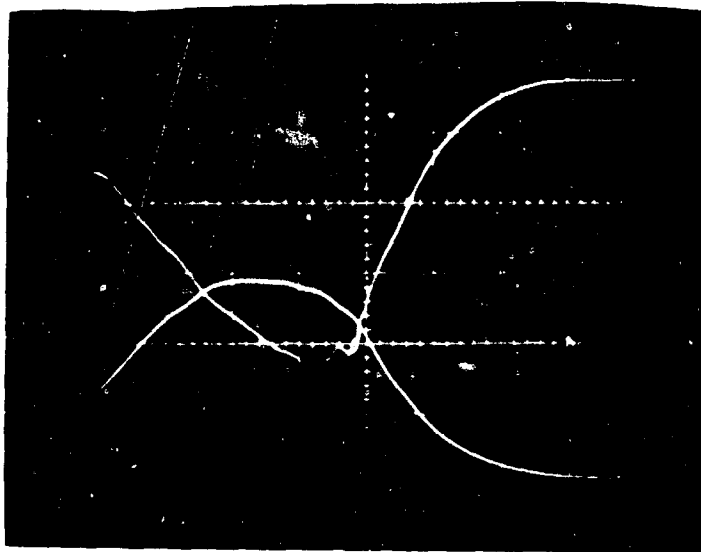
Oscilloscope trace showing voltage and
current output of 1" x 4" explosive driven
MHD generator.   Sweep speed 10 micro-
seconds/cm.   Upper trace is output voltage
at 200 volts/cm, lower trace is current at
10, 700 amperes/cm.   For this experiment
the magnetic field was 2. 2 w/m^2 and the
channel was filled with 10 mm Hg of helium.
The initial value of the load resistance was
0. 0201 ohms.

Figure
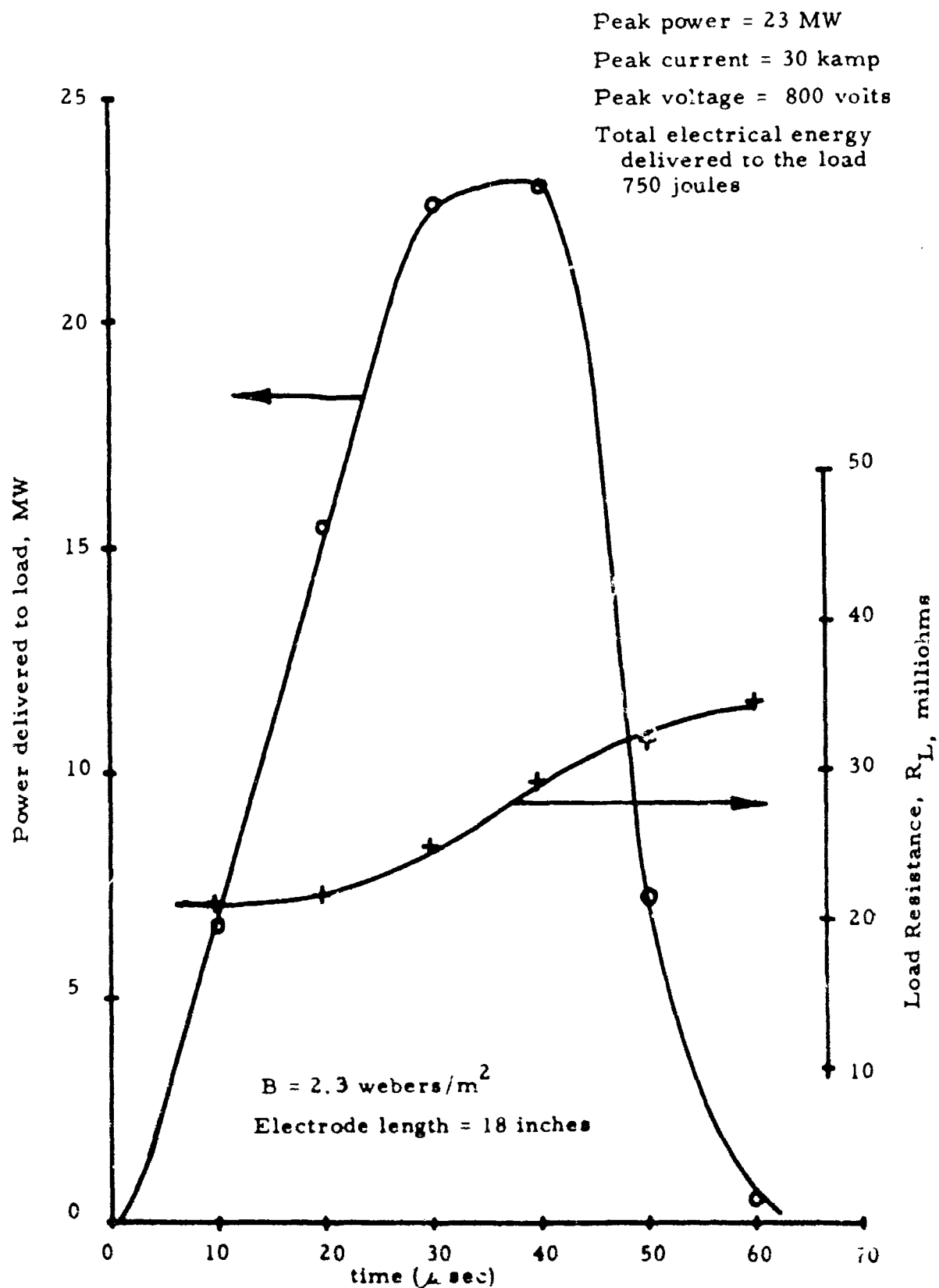
The electrical power excursion delivered to the load as a function of time from initial pickup for the 1 x 4 inch channel. The gas in the channel was helium at an initial pressure of 10 mm Hg. Also shown is the charge in the load resistance as a function of time due to the heating of the load.

Figure: 6

Power - MW

Load Resistance - milliohms

Air

Argon

Helium
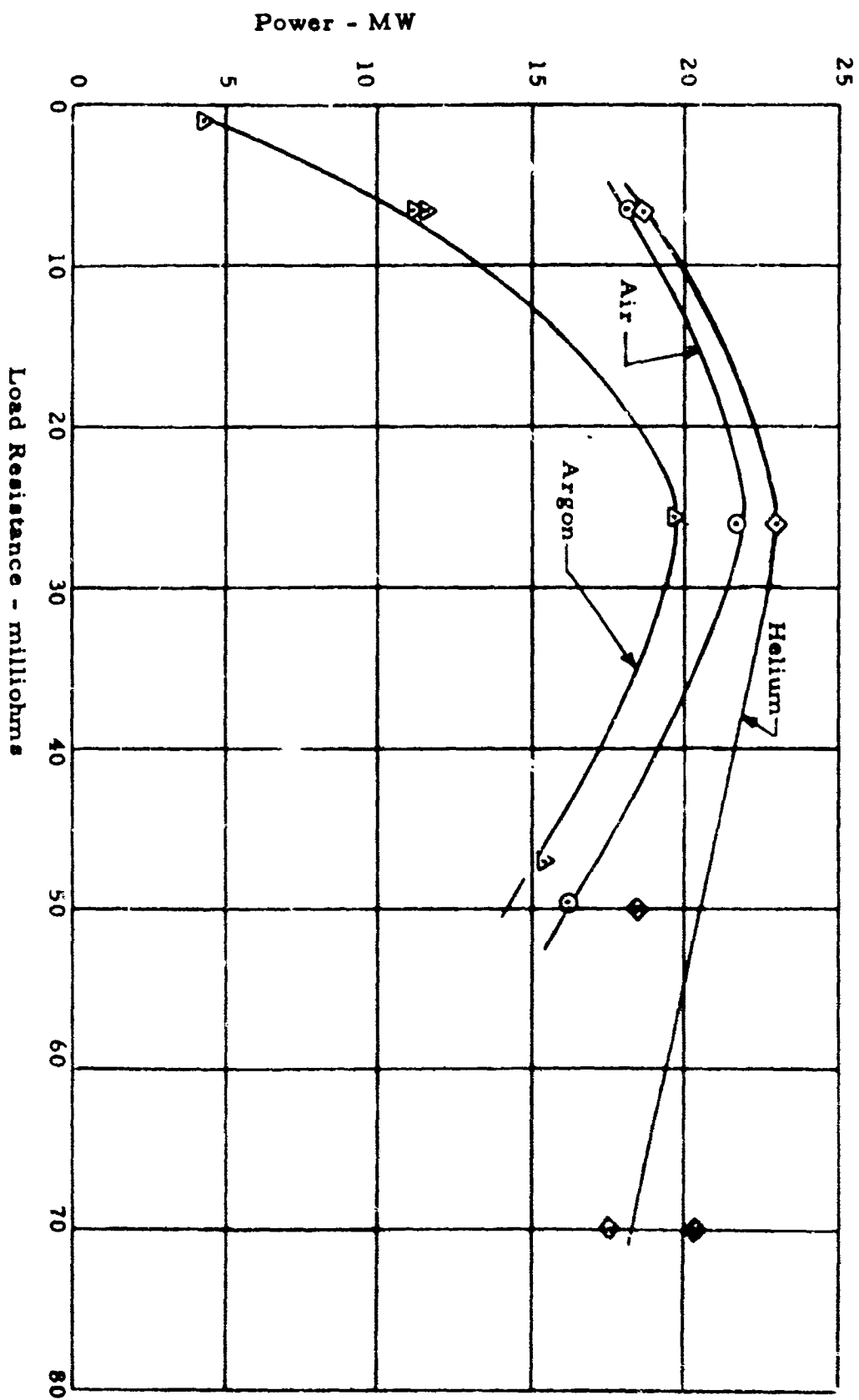
Figure 7. Power output of 1 inch by 4 inch explosive-driven MHD generator. Initial pressure, 10 mm Hg. Magnetic field, 2.3 w/m^2.

Power Output - MW

Load Resistance - Milliohms
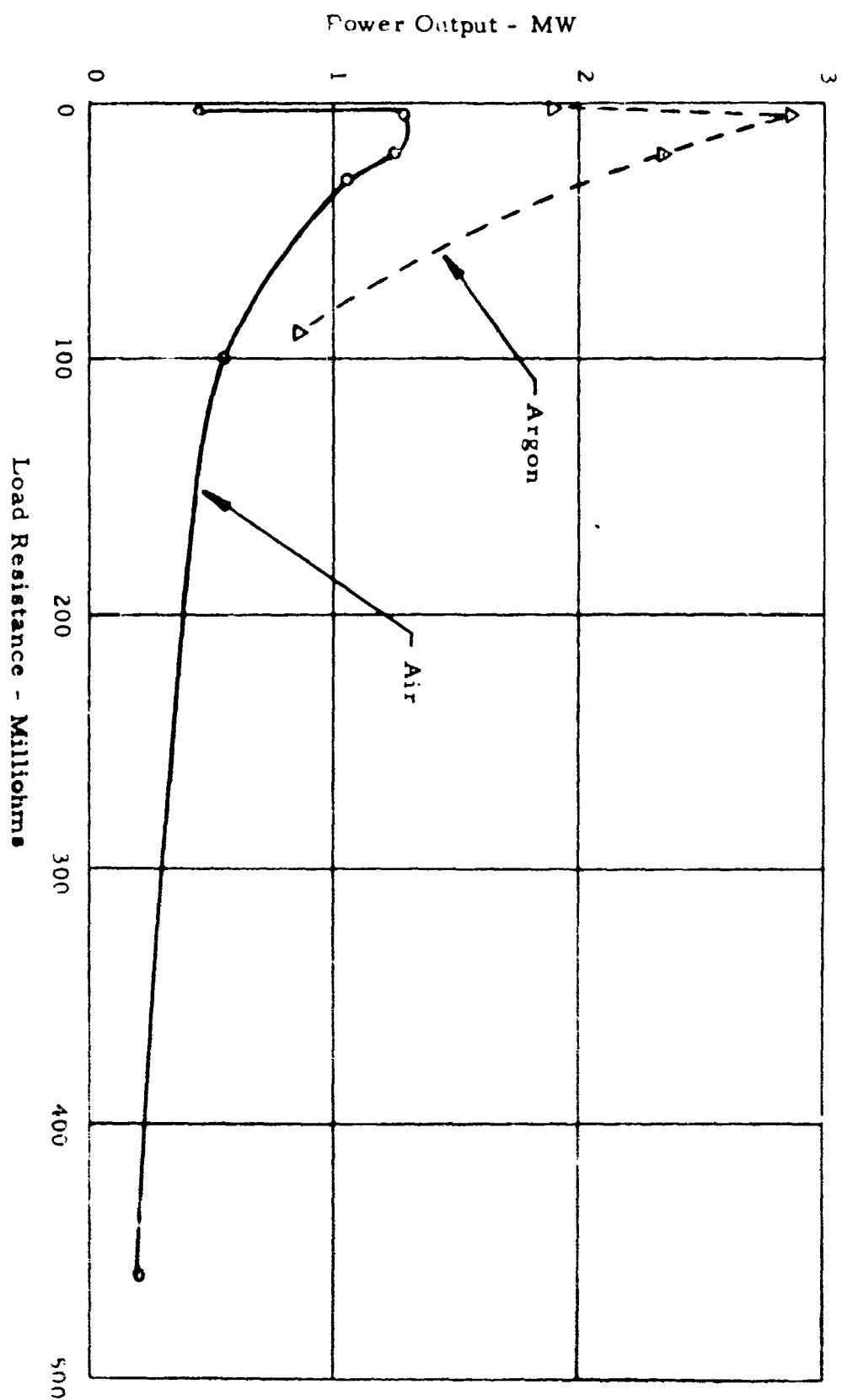
Figure 8

Power output as a function of load resistance for
1" x 1" explosive driven MHD generator with
initial pressure 10 mm Hg of either air or argon.
Magnetic field 1.7 W/M^2.

Initial Pressure
P_o (mm Hg)

760
700
500
300
100
10
0.1

1" Sq. CHANNEL

#8
#5
#3
#1

DISTANCE DOWN CHANNEL, X(cm)

Time, T (μsec)
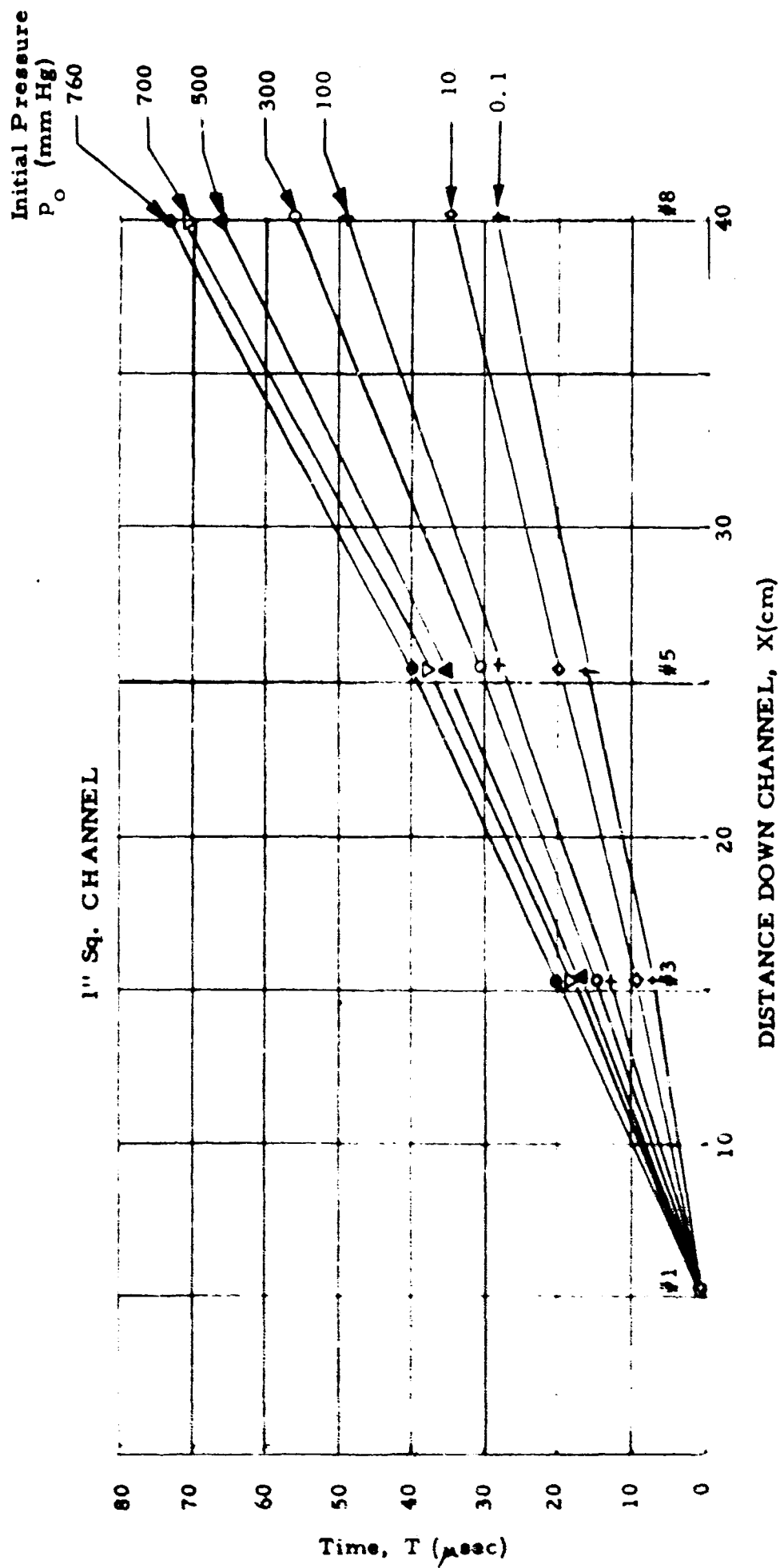
FIGURE 9

Front Arrival At Several Electrode Stations For Various Initial Pressures

Current - Amperes
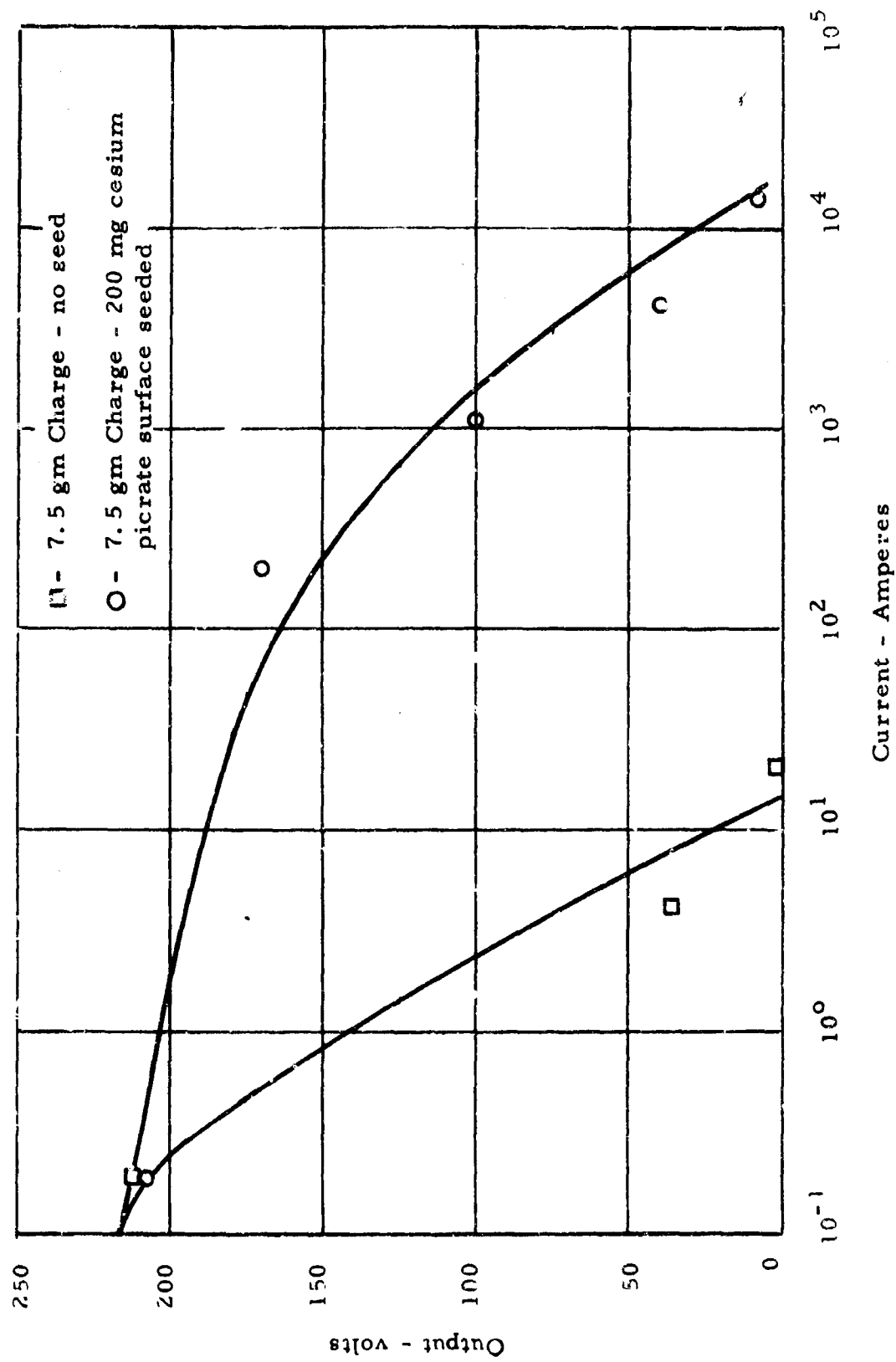
Figure 10

Comparison of seeded and non-seeded shaped charges in 1 inch by 1 inch explosive- driven MHD generator.

□ - 7.5 gm Charge - no seed

O - 7.5 gm Charge - 200 mg cesium picrate surface seeded

Figure

Typical oscilloscope trace from explosive driven MHD
generator. Upper trace is the voltage across 0.00945
ohm resistor, at 50 volts/cm gain. Lower trace is cur-
rent through load, gain is 1070 amperes/cm. Initial
pressure is 10 mm Hg, magnetic field 17 KG, and sweep
speed 2 μ sec/cm.
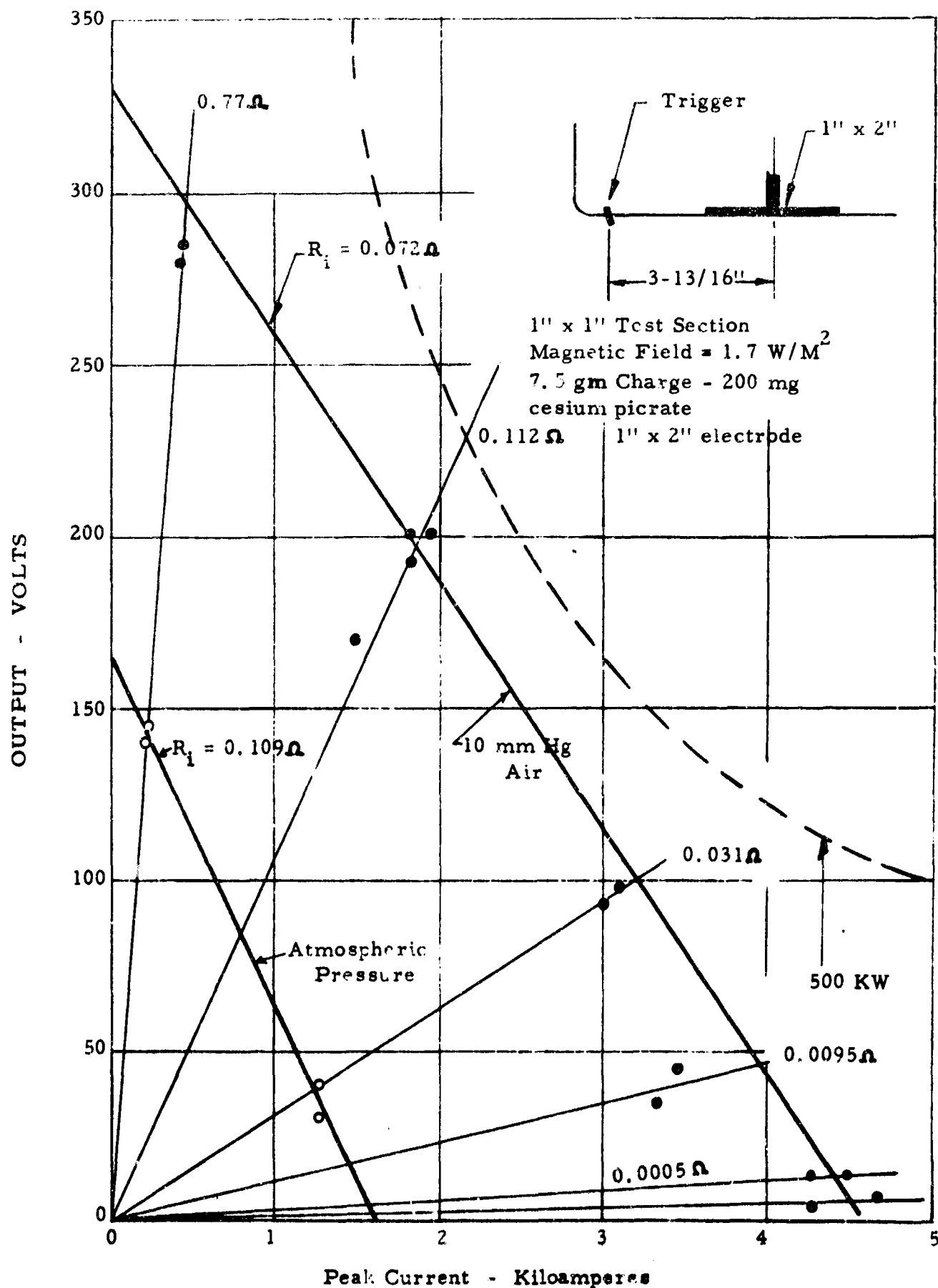
Figure 12

Voltage-Current characteristic of explosive
driven MHD generator for conductivity
determination.
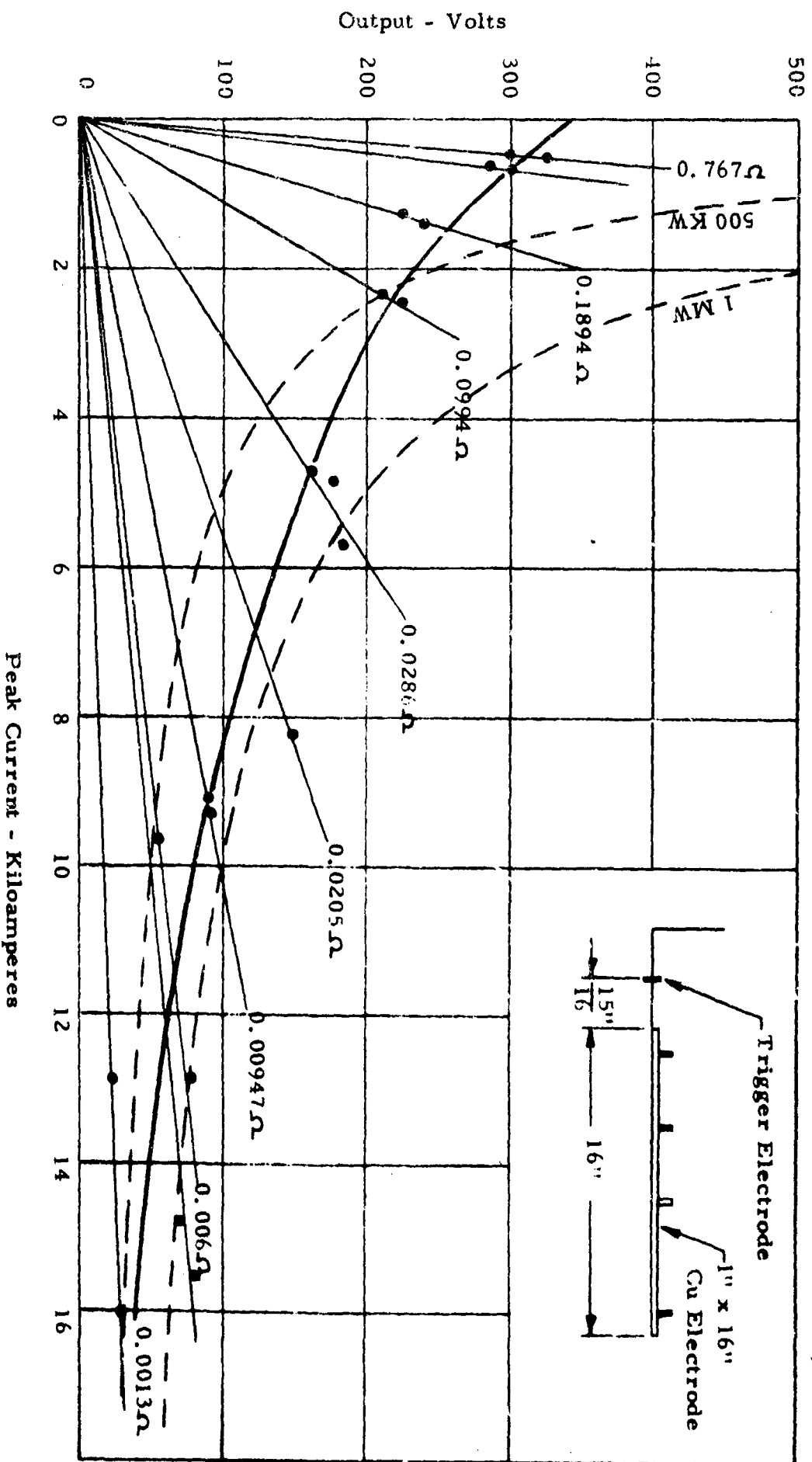
Output characteristics of 1 inch by 1 inch explosive-driven MHD channel for various load
resistances. Magnetic field 1.7 w/m², initial pressure 10 mm Hg, air.

Figure 13
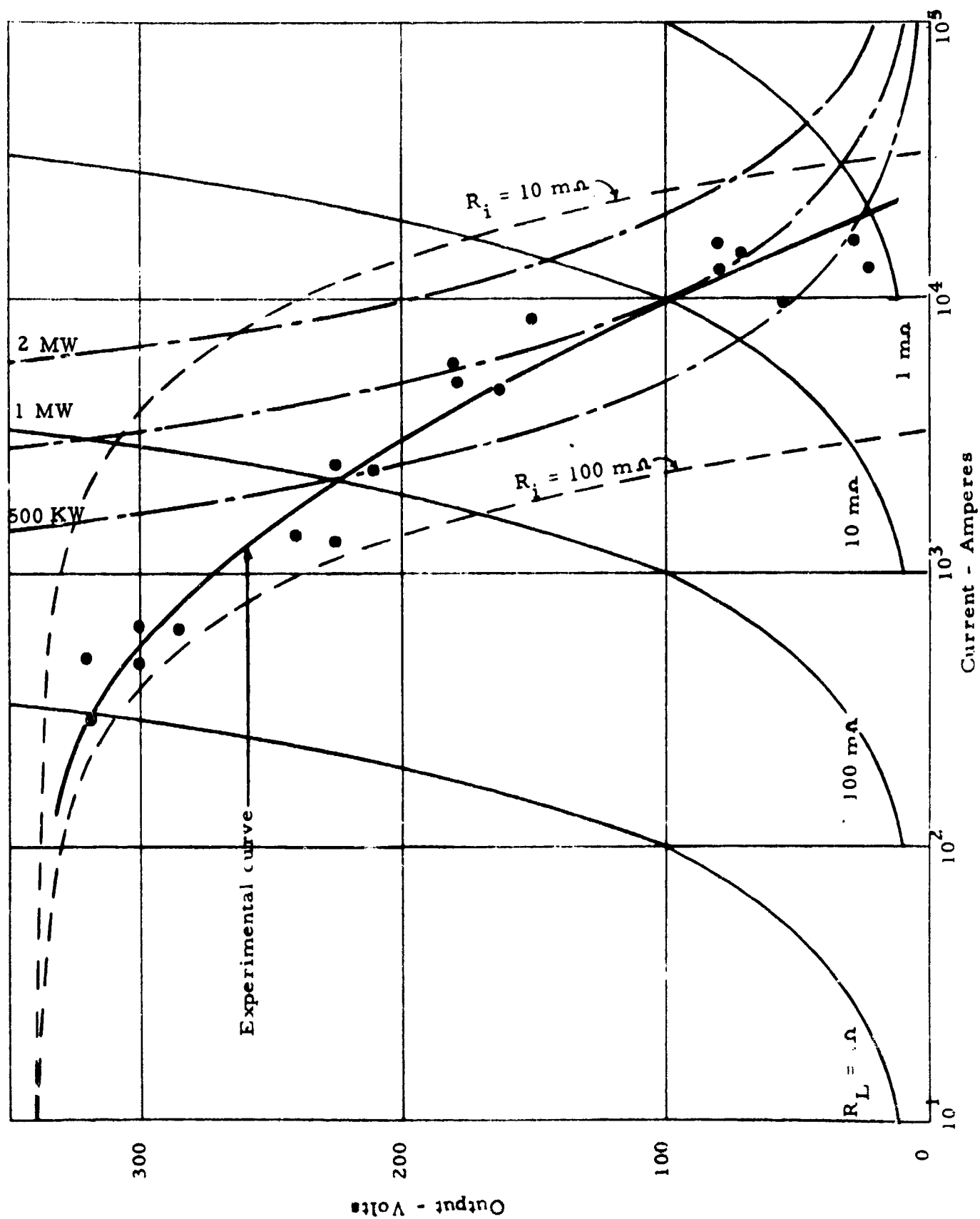
Figure 14

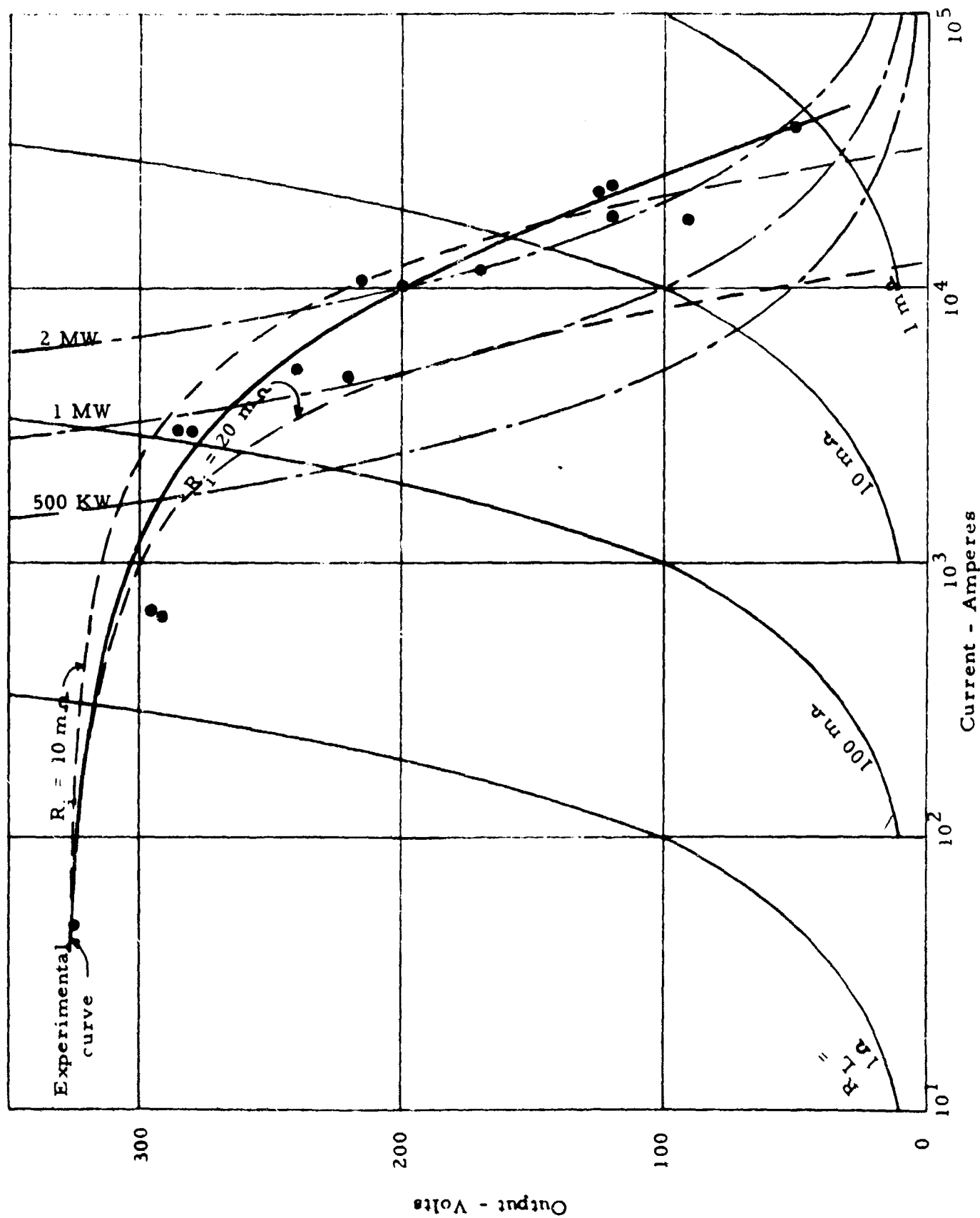Output voltage at peak current for the 1 inch x 1 inch channel at 10 mm Hg, air.

Figure 15

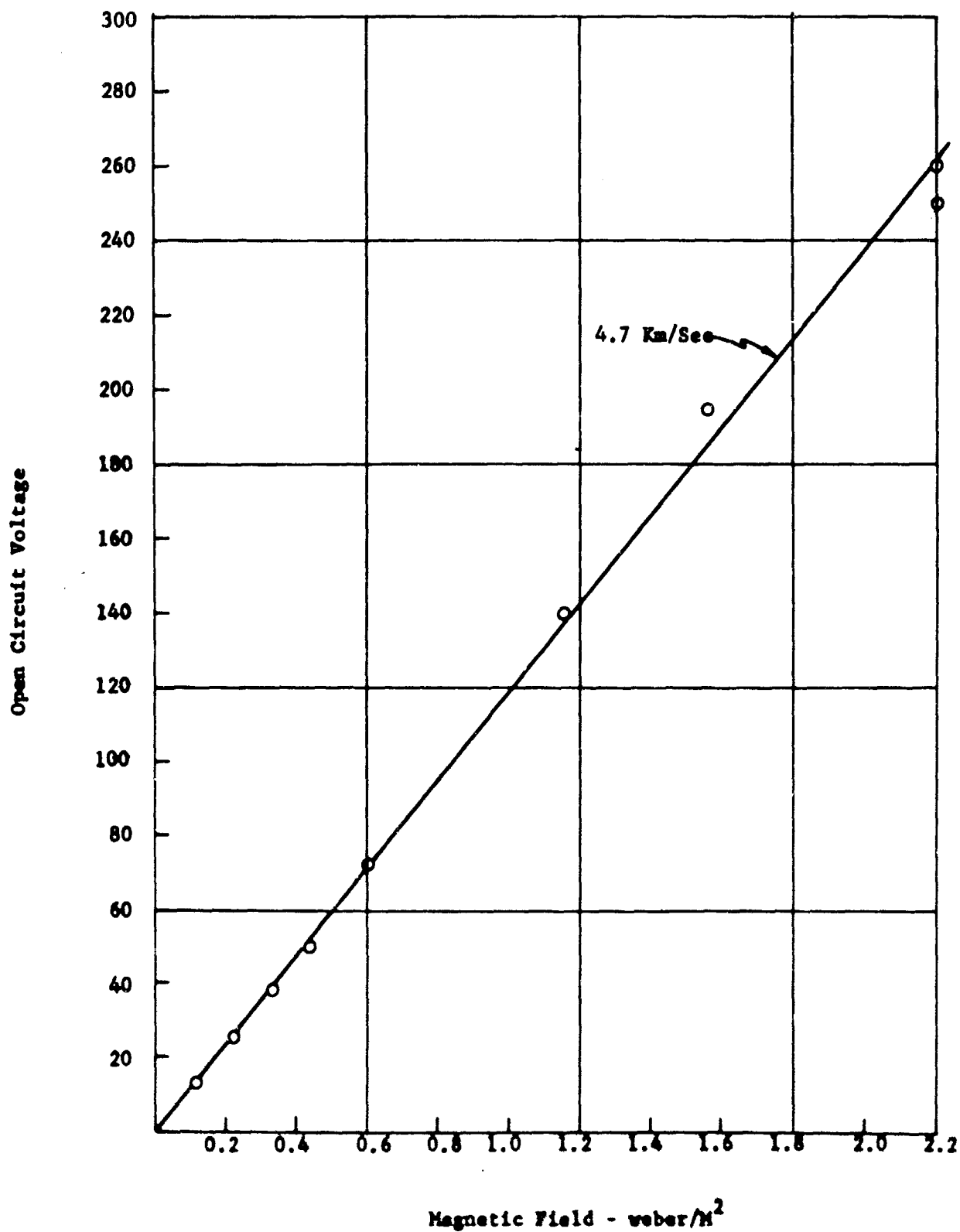Output voltage at peak current for the 1 inch x 1 inch channel at 10 mm Hg. argon.
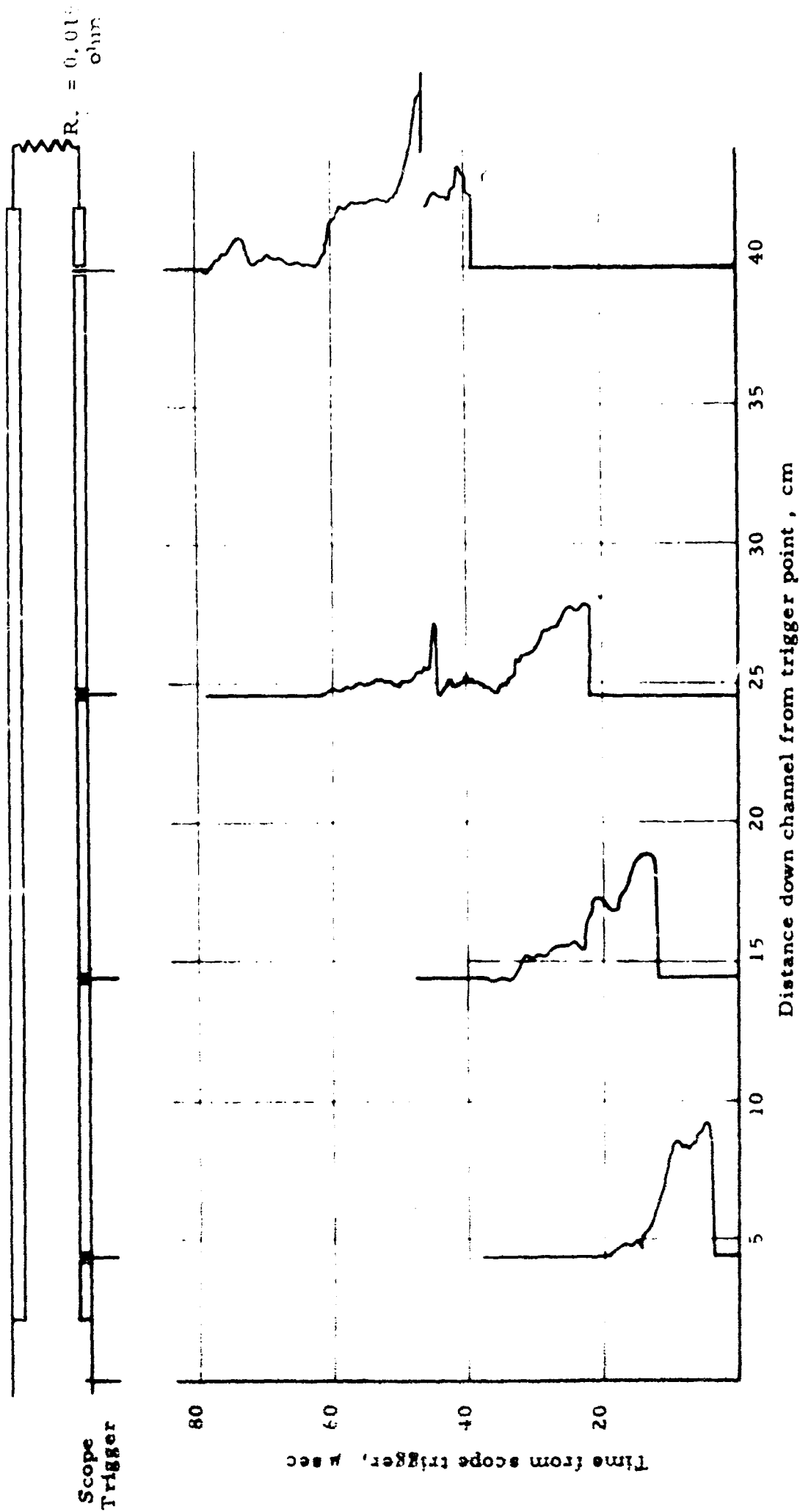
Figure 16. Open circuit voltage versus applied field. From this plot the effective gas velocity of 4.7 KM/sec can be determined.

Typical oscilloscope traces from four 1.5 mm dia. probes installed through the top electrode in the 1" x 1" explosive-driven MHD generator. The probes are connected to the scopes with 50 ohm terminated co-axial cables. Initial pressure in the test channel is 10 mm Hg. B = 17 KG. It is apparent how the conducting pulse widens with distance down the channel.

FIGURE: 17

Velocity Change - KM/sec

Electrical Output - Joules

+ Air
o Argon
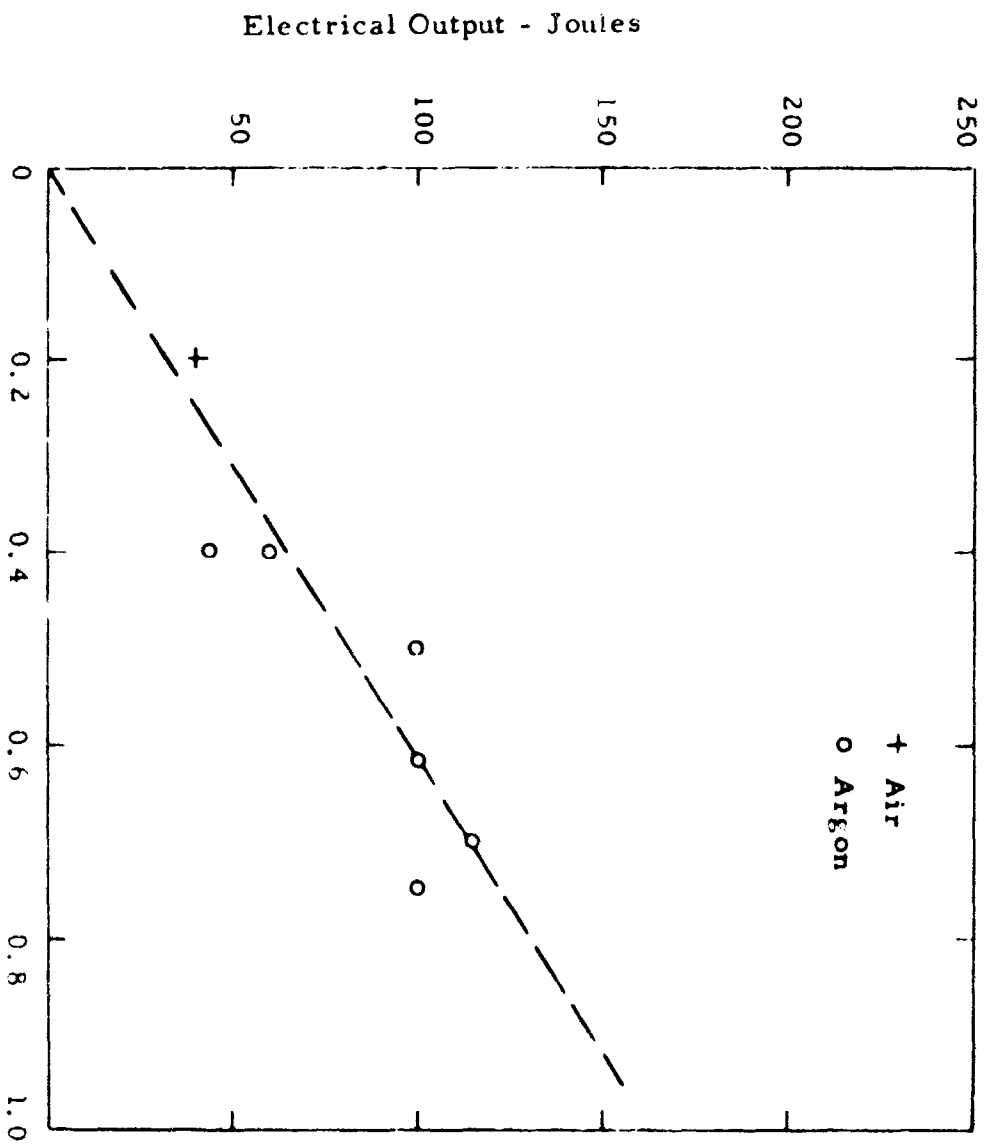
Change in velocity of conductive detonation products as a function of extracted energy in explosive-driven MHD generator. Generator channel is 1 inch by 1 inch, by 16 inches long. Magnetic field is 1.7 w/m². Average velocity without energy extraction is 10.4 km/sec.

Figure 18